Journal of Physics G: Nuclear and Particle Physics

PAPER

Approximate self-energy for Fermi systems with large s-wave scattering length: a step towards density functional theory

To cite this article: Antoine Boulet and Denis Lacroix 2019 *J. Phys. G: Nucl. Part. Phys.* **46** 105104

IOP Publishing Journal of Physics G: Nuclear and Particle Physics

J. Phys. G: Nucl. Part. Phys. **46** (2019) 105104 (30pp) https://doi.org/10.1088/1361-6471/ab2f0b

Approximate self-energy for Fermi systems with large s-wave scattering length: a step towards density functional theory

Antoine Boulet and Denis Lacroix

Institut de Physique Nucléaire, IN2P3-CNRS, Université Paris-Sud, Université Paris-Saclay, F-91406, Orsay Cedex, France

E-mail: boulet@ipno.in2p3.fr and lacroix@ipno.in2p3.fr

Received 15 February 2019, revised 13 June 2019
Accepted for publication 3 July 2019
Published 27 August 2019

Abstract

In the present work, we start from a minimal Hamiltonian for Fermi systems where the s-wave scattering is the only low energy constant (LEC) at play. The many-body perturbative approach that is usually valid at rather low density is first discussed. We then use the resummation technique with the ladder approximation to obtain compact expressions for both the energy and/or the on-shell self-energy in infinite spin-degenerated systems. The diagrammatic resummation technique has the advantage in general to be predictive in a region of density larger compared to many-body perturbation theory. It also leads to a non-diverging limit as $|a_s| \rightarrow +\infty$. Still, the obtained expressions are a rather complex function of the Fermi momentum k_F. We introduce the full phase-space or the partial phase-space approximations respectively applied to the energy or to the self-energy to simplify their dependences in terms of $(a_s k_F)$ while keeping the correct limit at low density and the non-diverging property at large $|a_s k_F|$. Quasi-particle properties of the Fermi system in various regimes of density and scattering length are then illustrated. Our conclusion is that such simplified expressions where the direct link is made with the LEC without fine-tuning can provide a clear guidance to obtain density functional theory (DFT) beyond the perturbative regime. However, quasi-particle properties close or near unitarity cannot be reproduced unless this limit is explicitly used as a constraint. We finally discuss how such approximate treatment of quasi-particles can guide the development of DFT for strongly interacting Fermi systems.

Keywords: energy density functional, Fermi systems, neutron matter, self-energy

(Some figures may appear in colour only in the online journal)

1. Introduction

Strongly interacting many-body Fermi systems can sometimes be described by rather simple density functional theories (DFT). This is the case of nuclear systems where simple functionals, like those based on the Skyrme type contact interactions [1–4], are nowadays widely used. With very few parameters, the functional can describe static, thermodynamical and dynamical properties very accurately in a unified framework. This is even more surprising in view of the complexity of the strong multi-body interaction between nucleons. The question (a) *'How such simplicity can emerge in strongly interacting Fermi systems?'* is still largely open in the nuclear physics community (see discussion in [5]).

This situation is not unique in nature. Simple DFTs apply also to the case of Fermi gas at unitarity. This gases are characterized by infinite s-wave scattering length a_s in the dilute regime. In this case, the energy becomes directly proportional to the free Fermi Gas energy. This situation can be seen as one of the simplest DFT one could ever imagine. Still, while in a DFT framework unitary gases can be described in a rather simplistic manner (see for instance [6–8]), their treatment starting from a particle–particle interactions, requires rather advanced many-body techniques like Monte-Carlo (MC) methods [9–15], Self-Consistent Green Function [16, 17], Brueckner Hartree–Fock (BHF) [18], Blod Diagrammatic MC [19, 20] eventually associated to resummation technique based on conformal-Borel transformation [21]. These approaches generally rely on rather involved numerical methods and usually prevent from connecting analytically the energy with the low-energy constants (LEC) associated to the underlying interaction. To our opinion, to reply to the question (a) it would be desirable to also give some hints on the other question (b) *'Can we qualitatively or quantitatively connect the parameters of the DFTs used in strongly interacting Fermions with the low-energy constants of the interaction?'* Assuming that we can directly connect the parameters used in a functional to the LEC of the interaction, this would render the DFT completely non-empirical. This would also be at variance with the strategy used nowadays to construct a DFT. Indeed, most currently used DFTs in cold atoms or in nuclei are usually directly adjusted either on experimental data or on pseudo-data obtained using one of the *ab initio* methods mentioned above. Such direct fitting procedure is very powerful because it includes automatically complex many-body correlations in the DFT. It also leads in general to a very precise description of the global properties of Fermi systems. This is for instance the case in atomic nuclei were the precision on the ground state energy is better than 2%–3% for medium mass nuclei and goes down to 0.5% for heavy systems (see for instance [22, 23]). This strategy has also some drawbacks. Among them, we usually face the difficulty that some components of the functional are not really constrained by the experiments. This is for instance the case of the density dependence of the symmetry energy in nuclei that is particularly important for the physics of exotic nuclei. Another example that was pointed out recently is the failure of empirical functionals to properly describe the low density limit of neutron matter [24]. One should mention that, with recent progresses in the nuclear interaction and in *ab initio* many-body techniques, there is an increasing interest in developing DFTs directly starting from a clear many-body framework. Among the recent works, we mention the Density Matrix Expansion proposed already some time ago [25, 26] that has reached now a certain level of maturity [27–32]. Another clearly defined approach is to write the effective action and use the inversion method as proposed in [33, 34] (see also the recent interesting progress of [35]). Still, the quantitative description of strongly interacting systems beyond the low density limit and/or beyond the Hartree–Fock approximation is a rather difficult task.

For this reason, we explore here qualitatively how a DFT can be obtained for three dimensional infinite Fermi systems where the parameters of the DFT are directly linked to the LEC of the interaction. More specifically, we consider the simplified problem where the interaction is described by a single LEC, a_s, and where the interaction strength can vary from the perturbative to the non-perturbative regime. Such physical situation was explored in different regimes using standard many-body techniques starting from an Effective-Field-Theory approach [36, 37]. For instance, the low density limit was studied in [38]. This case is particularly highlighting since in this case, up to third order in perturbation, the energy can be written as a simple polynomial (and potentially polylogarithmic from fourth order) of $\rho^{1/3}$ where ρ denotes the density. The perturbative approach breaks down when $(a_s k_{\rm F})$ increases. In this case, DFT have also been obtained using diagrammatic resummation techniques [39, 40]. Both perturbation and resummation to obtain compact expressions of the energy in terms of $(a_s k_{\rm F})$ will be briefly discussed here. As we will see, the brute-force resummation however generally suffers from the lack of predictive power especially close to the unitary limit. Following [39], we show that, using a procedure called hereafter phase-space approximation, the energy can be written as a simplified functional of $(a_s k_{\rm F})$ that in addition improves the description of strongly interacting systems. The work of [39] was actually the starting point of several new developments in the nuclear many-body context. In [24], guided by the simplified expression of the energy, a hybrid functional was proposed where some of the parameters are directly connected to a_s. Similarly, in [8, 41], a non-empirical functional was proposed that could reproduce both cold atoms gases and neutron matter up to $\rho \simeq 0.01\ \mathrm{fm}^{-3}$ including the effective range effect. Such new functionals were also used in [41] (see figure 6 of this reference) to understand the quantitative values of parameters that are used in empirical functional like Skyrme DFT. It was shown that the LEC are strongly renormalized due to in-medium effects. This actually was also recently shown using BHF in [42] and was encoded in the ELYO functional through density dependent coupling constants in [43]. A review on the novel scientific activities in this field can be found in [44] (see also the recent work [45] for application to finite systems including pairing).

The thermodynamical properties of strongly interacting systems was studied in [46] using one of the functional proposed recently. While most of the observed properties of systems close to unitarity were reproduced very accurately, two difficulties have been identified. The first one is that the dynamical response function in the superfluid phase can without surprise only be achieved by introducing explicitly the pairing field in the functional. The explicit treatment of superfluidity is not the subject of the present work and we will concentrate on normal systems. A second source of difficulty is the absence of clear prescription for the effective mass in the large a_s limit. Such effective mass and more generally quasi-particle properties are rather standard quantities helping to understand Fermi liquids. Its knowledge are of particular importance for instance to understand certain properties like the static response of neutron matter recently calculated with an *ab initio* theory in [47, 48]. It turns out, for instance for neutron matter, that the effective mass in neutron systems is scarcely known (see figure 6 of [46]) and has only been very recently estimated using Auxiliary-Field Diffusion MC in [49] and BHF calculation [50, 51]. For this reason, we also explore the possibility to obtain self-energies, for which direct contact with the Fermi liquid theory can be made, as functionals of $(a_s k_{\rm F})$ in the non-perturbative regime. In order to achieve this goal, we also use resummation techniques and extend the phase-space approximation to the self-energy. Finally, we briefly discuss how such analytical form can be useful in DFT approach.

2. DFT for dilute systems from many-body perturbation theory

We concentrate here on systems where the only LEC at play is the s-wave scattering length a_s. Infinite systems composed of spin-degenerated particles of mass m, i.e. a relevant situation for non-polarized neutron matter and/or spin degenerated cold atoms, are investigated. Following [38] and using the Effective-Field Theory (EFT) approach for homogeneous dilute Fermi gas, the s-wave interaction is simply written as a zero-range interaction that identifies with a constant in momentum space:

$$\langle \boldsymbol{k}'|V_{\mathrm{EFT}}|\boldsymbol{k}\rangle = C_0, \tag{1}$$

where $\boldsymbol{k}$ and $\boldsymbol{k}'$ are the relative momenta of the incoming and outgoing particles. The constant C_0 is linked to the scattering length a_s through ($\hbar = 1$):

$$C_0 = \frac{4\pi a_s}{m}, \tag{2}$$

using the convention that a negative a_s is attractive, so that the s-wave scattering phase shift δ_s verifies $k \cot \delta_s = -1/a_s$. The model case, where the interaction is dominated by a_s has been widely exploited in Fermi systems in the past [52–56] (see also [57]). The interaction (1) has a well-known ultra-violet (UV) divergence. In the present sections, we summarize some known results for this model. Note that, the results have been obtained with proper treatment of the UV divergence using standard techniques (in particular minimal subtraction scheme of dimensional regularization). For more details see [58–64] as well as the extensive discussion in [65].

Starting from the standard particle–hole representation of the propagator and following [38], it is possible within the EFT to obtain a systematic perturbative expansion of the energy of an homogeneous spin degenerated gas as

$$\frac{E}{E_{\mathrm{FG}}} = 1 + \frac{E^{(1)}}{E_{\mathrm{FG}}} + \frac{E^{(2)}}{E_{\mathrm{FG}}} + \frac{E^{(3)}}{E_{\mathrm{FG}}} + \cdots \tag{3}$$

$$= 1 + (g-1)\frac{10}{9\pi}(a_s k_{\mathrm{F}}) + (g-1)\frac{4}{21\pi^2}(11 - 2\ln 2)(a_s k_{\mathrm{F}})^2 + \cdots, \tag{4}$$

where $E^{(n)}$ denotes the contribution of the nth order in perturbation. $E_{\mathrm{FG}} = \frac{3}{5}\frac{k_{\mathrm{F}}^2}{2m}\rho$ denotes the Free-Gas (FG) energy at density ρ and where the degeneracy is here $g = 2$. The density is linked to the Fermi momentum k_{F} through $\rho = g(6\pi^2)^{-1}k_{\mathrm{F}}^3$. We recognize in (4) the Lee-Yang expansion [52–54], also obtained using EFT in [38] that is valid at low density when $(a_s k_{\mathrm{F}}) \ll 1$. Higher order contributions can be evaluated analytically (or numerically) in a similar way. For instance, the energy per particle at third order has been historically obtained by Efimov and Amusia [66, 67], Baker [68] and Bishop [69] and was more recently discussed in different works [40, 70–75]. Very recently, the fourth order has also been worked out [76].

One shortcoming of the perturbative expansion given by equation (4) is that it has a rather limited range of application when the scattering length become anomalously large as it happens in cold atoms [77, 78] and/or neutron matter [57]. Unless the expansion is made up to infinity in equation (3), the deduced energy only applies below a certain maximum density. For instance, the s-wave scattering length for neutron-neutron or proton-proton interaction is $a_s \sim -20$ fm, leading to a range of validity in density $\rho \lesssim 10^{-6}\,\mathrm{fm}^{-3}$ for the perturbative expansion. Compared to the saturation density $\rho_0 \sim 0.16\,\mathrm{fm}^{-3}$, i.e. typical density in nuclear system, the perturbation theory is not appropriate to describe properly these systems at the relevant density scale. In these cases, non-perturbative approaches are mandatory.

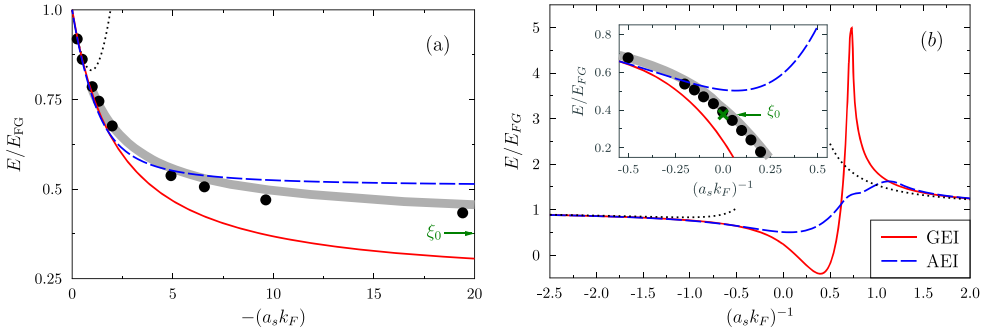

Figure 1. Energy in unit of the free Fermi gas energy as function of (a) $-(a_s k_F)$ and (b) $(a_s k_F)^{-1}$. The red solid and blue dashed lines are, respectively, obtained by direct numerical integration of equations (5) and (6). For reference, the black dotted line corresponds to the Lee-Yang formula obtained by truncating equation (4) at second order. In both panels, the grey area indicates the result obtained by fitting the experiment [83] with a Padé approximation while the black circles are the Diffusion Monte-Carlo (DMC) results or [13]. In the inset of panel (b), a focus is made near unitarity. In all panels, the arrow indicates the value of the Bertsch parameter $\xi_0 = 0.37$.

3. Diagrammatic resummation technique for the energy

Motivated by systems with anomalously large scattering lengths, several strategies have been proposed for selecting certain classes of diagrams and for providing compact expressions of the energy in terms of $(a_s k_F)$. Starting from the seminal work of [70], several attempts have been made to obtain compact expression of the energy as a phase-space integral where selected class of diagrams are summed to all order. Detailed discussion on diagrammatic many-body approaches can be found in [79, 80] and specific aspects of the nuclear many-body problem are reviewed in [81]. Here, we give two examples that will be the starting point of the work made in the work presented in this article. Retaining only the particle–particle (pp) ladder diagrams and after averaging over angles and using the minimal subtraction scheme of dimensional regularization [58–64], the energy can be written as (see for instance [39, 40, 70] and appendix A for the definition of s and t):

$$\frac{E}{E_{\rm FG}} = 1 + \frac{80}{\pi}\int_0^1 s^2 {\rm d}s \int_0^{\sqrt{1-s^2}} t{\rm d}t \, \frac{(a_s k_{\rm F}) I(s,\, t)}{1 - (a_s k_{\rm F}/\pi) F(s,\, t)}. \tag{5}$$

Alternatively, using in-medium propagator where both particle–particle (pp) and hole–hole (hh) propagators are accounted for simultaneously, the energy has been recast as [40, 82]:

$$\frac{E}{E_{\rm FG}} = 1 + \frac{80}{\pi}\int_0^1 s^2 {\rm d}s \int_0^{\sqrt{1-s^2}} t{\rm d}t \, \arctan \frac{(a_s k_{\rm F}) I(s,\, t)}{1 - (a_s k_{\rm F}/\pi) R(s,\, t)}. \tag{6}$$

The explicit forms of the functions I, F, and R are given in appendix A. In the following, results of the numerical integrations of equations (5) and (6) will be referred as *Geometric series Exact Integration* (GEI) and *Arctangent series Exact Integration* (AEI), respectively. Both equations (5) and (6) present several interesting features compared to a perturbative expansion. Firstly, they could be expanded in powers of $(a_s k_F)$ and, noteworthy, their second order expansions match the Lee-Yang formula. We show in figure 1(a) a comparison of the

energy obtained by integrating numerically the two resummed expressions as a function of $(a_s k_F)$.

One of the motivations for the use of resummation is that, contrary to any truncation at a given order in perturbation the energy is not diverging as $|a_s k_F| \to +\infty$, i.e. in the unitary gas regime (see panel (b) of figure 1). This was firstly discussed in [39] for the GEI case and latter in [40] for the AEI case. As noted in these works, the ratio:

$$\xi_0 = \lim_{|a_s k_F| \to +\infty} \frac{E}{E_{FG}} \tag{7}$$

generally refereed to as the Berstch parameter, significantly depends on the class of diagrams selected for resummation. In the two cases considered here, we have:

$$\xi_{GEI} \simeq 0.24 \qquad \text{and} \qquad \xi_{AEI} \simeq 0.51. \tag{8}$$

These values in both cases significantly differ from the experimentally observed value of the Bertsch parameter $\xi_0 = 0.37$ [13, 17, 83, 84]. It should be however kept in mind that the value of ξ_0 corresponds to the one of a superfluid unitary gas while superfluidity is not accounted for in the present resummation. Therefore, to be consistent, one should *a priori* compare with the value of the Bertsch parameter in normal systems. In [18], using BHF approach, a value 0.507 was found, which is compatible with the experimental result of [84] giving 0.45. This value is actually consistent with the AEI case given by equation (6). Nevertheless, one obvious conclusion is that the choice of certain diagrams significantly affects the energy behavior as $(a_s k_F)$ increases.

3.1. Phase-space approximation for the resummed energy

Despite the fact that the selection of diagrams influences the results of a resummation approach, the resulting expressions of the energy in terms of $(a_s k_F)$ is an interesting steps towards a DFT for interacting systems beyond the Lee-Yang formula. Still, the deduced expressions are rather complicated especially due to the necessity to perform explicit integrations on phase-space for all values of k_F (note also that k_F also appears in the definition of s and t, see appendix A). This complexity can however be partially reduced using what we call below a Phase-Space (PS) approximation. The PS approximation was discussed for the Geometric series case in [39], it consists simply in replacing the numerator and denominator entering in the integral, respectively, by their average values integrated over the phase-space, leading in this way to a much simpler approximation. Let us introduce the notation $\langle\langle X \rangle\rangle$ defined as:

$$\langle\langle X \rangle\rangle \equiv \int_0^1 s^2 \mathrm{d}s \int_0^{\sqrt{1-s^2}} t \mathrm{d}t X(s, t).$$

We see for instance that the GEI can be written as:

$$\begin{aligned} \frac{E}{E_{FG}} &= 1 + \frac{80}{\pi} \left\langle \left\langle \frac{(a_s k_F) I}{1 - (a_s k_F/\pi) F} \right\rangle \right\rangle \\ &= 1 + \frac{80}{\pi} (a_s k_F) \langle\langle I \rangle\rangle \left\{ 1 + \frac{(a_s k_F)}{\pi} \frac{\langle\langle IF \rangle\rangle}{\langle\langle I \rangle\rangle} + \frac{(a_s k_F)^2}{\pi^2} \frac{\langle\langle IF^2 \rangle\rangle}{\langle\langle I \rangle\rangle} + \cdots \right\}. \end{aligned} \tag{9}$$

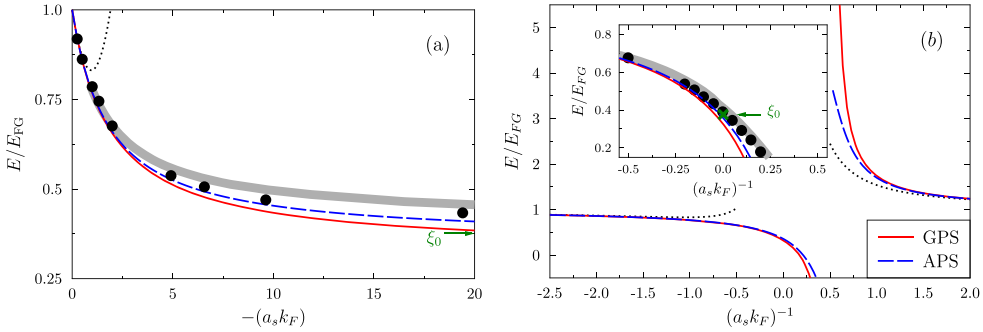

Figure 2. Same as figure 1 using the GPS (red solid line) and APS (blue dashed line) approximation.

The PS approximation consists of replacing this expression simply assuming:

$$\frac{E}{E_{\rm FG}} \simeq 1 + \frac{80}{\pi}(a_s k_{\rm F})\langle\langle I\rangle\rangle\left\{1 + \frac{(a_s k_{\rm F})}{\pi}\frac{\langle\langle IF\rangle\rangle}{\langle\langle I\rangle\rangle} + \frac{(a_s k_{\rm F})^2}{\pi^2}\frac{\langle\langle IF\rangle\rangle^2}{\langle\langle I\rangle\rangle^2} + \cdots\right\}$$
$$= 1 + \frac{80}{\pi}\frac{(a_s k_{\rm F})\langle\langle I\rangle\rangle}{1 - (a_s k_{\rm F}/\pi)\langle\langle IF\rangle\rangle/\langle\langle I\rangle\rangle}. \tag{10}$$

This approximation still insures that the Lee-Yang expression is recovered up to second order in $(a_s k_{\rm F})$. Using the integrals given in appendix A.1, we obtain:

$$\frac{E}{E_{\rm FG}} = 1 + \frac{\frac{10}{9\pi}(a_s k_{\rm F})}{1 - \frac{6}{35\pi}(11 - 2\ln 2)(a_s k_{\rm F})}. \tag{11}$$

This compact form, called hereafter Geometric Phase-Space (GPS), was introduced at several occasions in the nuclear physics and/or cold atom context [39, 76, 85, 86]. The energy obtained in the GPS approximation is shown in figure 2.

Equation (11) could be interpreted as a minimal Padé approximation in $(a_s k_{\rm F})$ at low density, the Padé[1/1] recently shown for instance in figure 2 of [76]. We mention that Padé approximations Padé[k/k] can be obtained (see for instance [85]) that could reproduce the development (9) to a given desired order in $(a_s k_{\rm F})$ for any k.

One important conclusion for the present work is that the energy obtained from equation (11) largely extend the domain of density over which it reproduces the exact MC result compared to the Lee-Yang formula, i.e. compared to the second order perturbation theory. Essentially, above $-(a_s k_{\rm F}) = 1$ in figure 2, the Lee-Yang expression deviates significantly from the exact calculation. Note that the inclusion of third order perturbation theory only slightly extend the domain of validity. On contrary, we see in figure 2(a) that the resummed formula follows closely the exact results and therefore it could be useful to obtain a compact form for a DFT beyond the perturbative regime. The GPS approximation has indeed been recently used in [24] to obtain a nuclear EDF where some of the parameters are directly connected to the physical s-wave scattering length, contrary to the widely used Skyrme EDF [2].

Although the main goal of the present work is to obtain DFT suitable beyond the perturbative regime, we would like to mention also that the approximated form (11) leads to a Bertsch parameter $\xi_{\rm GPS} = 0.32$, that is closer to the one obtain at unitarity for superfluid systems [24, 39] compared to the one obtained with direct integration. It should be noted

however that a relatively small difference in the value of ξ_0 leads to large deviations in the energy due to the fact that it is multiplied by the Free-Gas energy. For this reason, it was proposed in equation (9) to relax the slightly the low density constraint and adjust directly the denominator on the unitary gas in [8, 87]. Such strategy turns out to be highly predictive for systems close and/or at unitarity [41, 46].

3.2. Phase-space approximation with arctangent resummation (Ladder approximation)

Using the same approximation as above, a phase-space approximation of equation (6) can be obtained leading to the following compact expression, called hereafter *Arctangent Phase-Space* (APS):

$$\begin{aligned}\frac{E}{E_{\rm FG}} &= 1 + \frac{80}{\pi}\left\langle\left\langle \arctan\frac{(a_s k_{\rm F})I}{1-(a_s k_{\rm F}/\pi)R}\right\rangle\right\rangle \\ &= 1 + \frac{80}{\pi}\langle\langle 1\rangle\rangle\left\{(a_s k_{\rm F})\frac{\langle\langle I\rangle\rangle}{\langle\langle 1\rangle\rangle} + \frac{(a_s k_{\rm F})^2}{\pi}\frac{\langle\langle IR\rangle\rangle}{\langle\langle 1\rangle\rangle}\right. \\ &\quad \left. + \frac{(a_s k_{\rm F})^3}{\pi^2}\left[\frac{\langle\langle IR^2\rangle\rangle}{\langle\langle 1\rangle\rangle} - \frac{\pi^2}{3}\frac{\langle\langle I^3\rangle\rangle}{\langle\langle 1\rangle\rangle}\right] + \cdots\right\} \\ &\simeq 1 + \frac{80}{\pi}\langle\langle 1\rangle\rangle\left\{(a_s k_{\rm F})\frac{\langle\langle I\rangle\rangle}{\langle\langle 1\rangle\rangle} + \frac{(a_s k_{\rm F})^2}{\pi}\frac{\langle\langle IR\rangle\rangle}{\langle\langle 1\rangle\rangle}\right. \\ &\quad \left. + \frac{(a_s k_{\rm F})^3}{\pi^2}\left[\frac{\langle\langle IR\rangle\rangle^2}{\langle\langle I\rangle\rangle\langle\langle 1\rangle\rangle} - \frac{\pi^2}{3}\frac{\langle\langle I\rangle\rangle^3}{\langle\langle 1\rangle\rangle^3}\right] + \cdots\right\}. \end{aligned} \tag{12}$$

Then, making the summation to all orders and using the integrals given in appendix A.1, we obtain:

$$\begin{aligned}\frac{E}{E_{\rm FG}} &= 1 + \frac{80}{\pi}\langle\langle 1\rangle\rangle \arctan\frac{(a_s k_{\rm F})\langle\langle I\rangle\rangle/\langle\langle 1\rangle\rangle}{1-(a_s k_{\rm F}/\pi)\langle\langle IR\rangle\rangle/\langle\langle I\rangle\rangle} \\ &= 1 + \frac{16}{3\pi}\arctan\frac{\frac{5}{24}(a_s k_{\rm F})}{1-\frac{6}{35\pi}(11-2\ln 2)(a_s k_{\rm F})}. \end{aligned} \tag{13}$$

Illustrations of the energy dependence obtained in the APS approximation are shown in figure 2. We note that the APS closely follow the GPS case at low density. This is indeed expected since both are constructed to match the same Lee-Yang expansion for low density Fermi gas. More surprisingly, the APS turns out to be very effective up to unitarity. It indeed gives a Bertsch parameter equal to $\xi_{\rm APS} \simeq 0.36$ that is very close to ξ_0. This is an interesting finding since, contrary to the GPS case where the unitary limit can only be reproduce at the price of degrading the description of the low density regime, in the APS case, both low density (second order expansion in $(a_s k_{\rm F})$) and unitary limit can be very reasonably accounted for without adjusting any parameter. Note that similarly to the geometric series case, one might eventually replace the constant appearing in the denominator of equation (13) by a free parameter adjusted to reproduce the unitary gas limit.

The two approximations (GSP, APS) introduced here are rather simple functions of $k_{\rm F}$ compared to the original GEI, AEI integral equations and therefore provide much simpler functionals of the density ρ. One should mention a drawback of the phase-space approximation (see figure 2). By using phase-space approximation in the denominator, one restrict the value of $(a_s k_{\rm F})$ that could be used. Indeed, while the integrated GEI and/or AEI integral

forms can be applied from negative to positive values of a_s around unitarity, this is not the case for the phase-space expressions where a pole appears for a certain positive value of a_s. From now on, we will only consider the case where a_s is negative that is also the relevant situation for neutron matter.

In summary, we have shown here that several functionals can be obtained that reproduce quite well the energy of Fermi gases at unitarity. We would like to mention that the value $\xi_0 = 0.37$ is the admitted value of *superfluid* unitary gas. It might then be surprising to reproduce this value with a functional originally motivated by the diagrammatic expansions of [40, 82] where superfluidity is not treated. It is however important to keep in mind that whatever is the motivation/strategy to produce a DFT, the only final criteria is the ability of the functional to accurately describe the ground-state energy of the system at various densities. This is actually the only purpose of a DFT constructed in the spirit of the original work of Hohenberg and Kohn who have shown the existence of a functional able to reproduce the exact energy consistently with the exact local one-body density [88, 89].

In the following, however we would like to consider directly the self-energy that is *a priori* clearly beyond the scope of a DFT approach. In this case, the discussion made above for the energy cannot be made and superfluidity should be explicitly introduced to describe superfluid systems. Such a treatment is beyond the scope of the present work and in the rest of the article, we will concentrate on non-superfluid systems.

4. Diagrammatic resummation for the self-energy

As noted in [46], functionals that do not explicitly use the concept of effective masses and/or pairing gap will have difficulties to reproduce the excitation properties in strongly interacting Fermi systems. This is one of the main motivation of the present work. Starting from a many-body diagrammatic approach based on Green functions, a natural way to make connection with the Fermi liquid theory is to use the concept of self-energy [57]. We concentrate here on non-superfluid systems. Similarly to the energy case, the resummation of the contribution of selected diagrams to all order can be made at the level of the self-energy. This was done for instance in [82] (see also [65] for a complete discussion). We only give here the resulting self-energies when either only pp diagrams or the pp and hh diagrams are retained. After resummation, the self-energy can be written as (again with the convention $p = k/k_{\rm F}$)[1]:

$$\frac{\Sigma(k)}{\mu_{FG}} = \Theta(k_{\rm F} - k)\int_0^1 s^2 {\rm d}s \int_0^{\sqrt{1-s^2}} t{\rm d}t\ \mathcal{S}(s,\, t,\, p) + \Theta(k - k_{\rm F})\int_0^{(1+p)/2} s^2 {\rm d}s \int_0^{(1+p)/2} t{\rm d}t\ \mathcal{S}'(s,\, t,\, p). \tag{14}$$

Here $\mathcal{S}$ and $\mathcal{S}'$ take different forms depending on the type of diagrams that are used. To avoid confusion between these two cases we will use the following convention: $\Sigma(k) = U(k) + {\rm i}W(k)$ for the self-energy obtained from the resummation of combined pp and hh ladder diagrams and $\Sigma_{\rm pp}(k) = U_{\rm pp}(k) + {\rm i}W_{\rm pp}(k)$ for the one where only pp ladder diagrams are used. The real and imaginary parts of the self-energy enter into the single-particle (sp) energy $\varepsilon(k)$ and the lifetime $\gamma(k)$ of the quasi-particle (qp), respectively. Similarly to the self-energy that could be separated into a real and imaginary part, we can decompose $\mathcal{S}$ and $\mathcal{S}'$ as:

[1] Note that, here, off-shell effects are neglected and we use the compact notation $\Sigma(k) \equiv \Sigma(\mathbf{k},\, \omega_k)$ where $\omega_k = \mathbf{k}^2/(2m)$.

$$\mathcal{S}^{(')} = \mathcal{U}^{(')} + \mathrm{i}\mathcal{W}^{(')} \quad \text{(pp and hh ladder diagrams)},$$
$$\mathcal{S}^{(')}_{\mathrm{pp}} = \mathcal{U}^{(')}_{\mathrm{pp}} + \mathrm{i}\mathcal{W}^{(')}_{\mathrm{pp}} \quad \text{(pp ladder diagrams only)}.$$

The expressions of these functions are given in appendix B.1. The resummed self-energies of [82] have a number of interesting properties.

First, for the two classes of selected diagrams considered here, in the low density regime, the first and second order self-energies given by equation (16) are properly recovered by construction. More precisely, expanding the self-energy in powers of $(a_s k_{\mathrm{F}})$, we obtain:

$$\frac{\Sigma(k)}{\mu_{\mathrm{FG}}} = \frac{\Sigma^{(1)}(k)}{\mu_{\mathrm{FG}}} + \frac{\Sigma^{(2)}(k)}{\mu_{\mathrm{FG}}} + \cdots \tag{15}$$

$$= \frac{4}{3\pi}(a_s k_{\mathrm{F}}) + (a_s k_{\mathrm{F}})^2[\Phi_2(p) + \mathrm{i}\Omega_2(p)] + \cdots \tag{16}$$

Here, we have defined $\mu_{\mathrm{FG}} \equiv k_{\mathrm{F}}^2/(2m)$ and we introduced the reduced momentum $p = k/k_{\mathrm{F}}$. The two functions $\Phi_2(p)$ and $\Omega_2(p)$ are related, respectively, to the real and imaginary parts of the self-energy and are given in appendix B. Similar but slightly more general expressions were derived in [90] by Galitskii (equations (34) and (35) of [90]) with the difference that the expansion was made with respect to a small parameter f_0 that identifies in the long wavelength limit to the s-wave scattering length (see also the discussion in chapter 4 of [57]). For the sake of simplicity, we will simply refer to equation (16) as the Galitskii formula in the following. Additional interesting discussions can be found in [91–94]. These references might also be useful to link eventually the present work with the theory of Fermi liquids. In particular, it would be interesting in the near future to investigate how the renormalization effect that is standardly employed in Landau Fermi liquid theory might be linked to the resummation technique used here.

Below, we will essentially focus here on the real part of the self-energy. The quasi-particle properties can be obtained from the behavior of the self-energy close to $k = k_{\mathrm{F}}$ $(p = 1)$ [95]. For instance, the chemical potential μ and the effective mass m^* are, respectively, linked to the value of $U(k)$ and its derivative at $k = k_{\mathrm{F}}$:

$$\mu = \frac{k_{\mathrm{F}}^2}{2m} + U(k_{\mathrm{F}}), \qquad \frac{m}{m^*} = 1 + \frac{m}{k_{\mathrm{F}}}\frac{\partial U(k)}{\partial k}\bigg|_{k=k_{\mathrm{F}}}. \tag{17}$$

Starting from the expansion (15) and making a Taylor expansion of each term around $k = k_{\mathrm{F}}$ (or $p = 1$), one obtains a systematic approach to compute quasi-particle properties in powers of $(a_s k_{\mathrm{F}})$. For instance, up to second order in $(a_s k_{\mathrm{F}})$[2]:

$$\begin{cases} \frac{\mu}{\mu_{\mathrm{FG}}} = 1 + \frac{4}{3\pi}(a_s k_{\mathrm{F}}) + \frac{4}{15\pi^2}(11 - 2\ln 2)(a_s k_{\mathrm{F}})^2 + \cdots \\ \frac{m^*}{m} = 1 + \frac{8}{15\pi^2}(7\ln 2 - 1)(a_s k_{\mathrm{F}})^2 + \cdots \end{cases} \tag{19}$$

These expressions are well known results also discussed in [90]. In particular, the latter equation is often referred to as the Galitskii mass formula.

[2] To obtain this result, we used the Taylor expansion:

$$\Phi_2(p) = \frac{4}{15\pi^2}(11 - 2\ln 2) - \frac{16}{15\pi^2}(7\ln 2 - 1)(p - 1) + \cdots \tag{18}$$

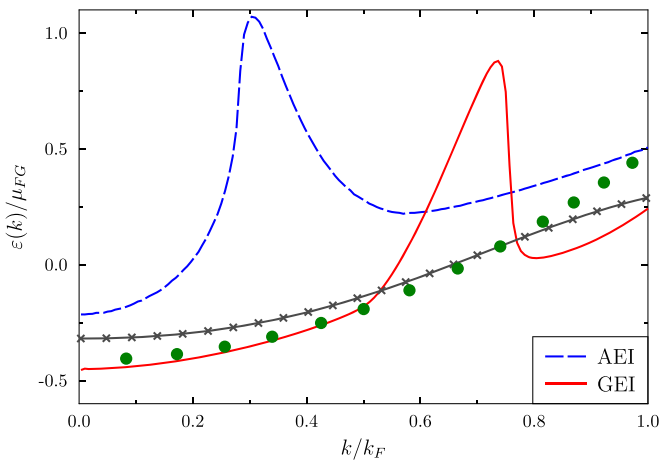

Figure 3. Single-particle energy as a function of $k/k_{\rm F}$ obtained at strict unitarity by direct integration of equation (14) with pp ladders only (red solid line) or both pp and hh ladders (blue dashed line). For comparison, the green circles correspond to the Brueckner Hartree–Fock calculation obtained without pairing effect [18] and the black crosses to the best fit of the experimental results obtained [96].

Another interesting feature of the expression given in appendix B, is that the self-energies do converge also to a finite result as $|a_s k_{\rm F}| \to +\infty$ for all k. This is illustrated in figure 3 where the results of direct integration of equation (14) are shown as a function of k at unitarity. Note that for the multidimensional numerical integration of the equations, we used the Vegas method implemented in the Cuba library [97]. The single-particle energies defined as:

$$\varepsilon(k) = \frac{k^2}{2m} + U(k), \tag{20}$$

and obtained in figure 3 coincides with those reported in [40] with marked bumps. These bumps seems unphysical not only because they significantly differ from the BHF calculations of [18] but also due to the presence of single-particle energies above the Fermi energy for $k < k_{\rm F}$. We would like to mention that there is no reason that the deduced self-energy is predictive at large scattering length due to the neglected diagrams. Another important remark is that the BHF calculations cannot also be regarded as exact and should be taken here as an illustration.

Starting from the different expressions, one can deduce from it, equation (17), the quasi-particle properties by direct numerical integration. We show in figure 4 the evolution of μ and m^*/m as a function of $(a_s k_{\rm F})$ obtained in the two types of resummation considered here. We see that both AEI and GEI approximation significantly extend the domain of validity compared to the perturbative theory and the corresponding chemical potential extracted from them are both rather close to the BHF result up to $|a_s k_{\rm F}| \simeq 2$–3. For the AEI case, it is remarkable to see, especially having in mind the strange behavior of figure 3, that the chemical potential extracted from the AEI case perfectly matches the BHF calculation for all regime of $(a_s k_{\rm F})$. We see however (panels (c) and (d) of figure 4) that the comparison is in general less favorable for the effective mass. Both approximations overpredict the effective mass compared to the BHF calculation for $|a_s k_{\rm F}| > 1$, even if the agreement is slightly better than the

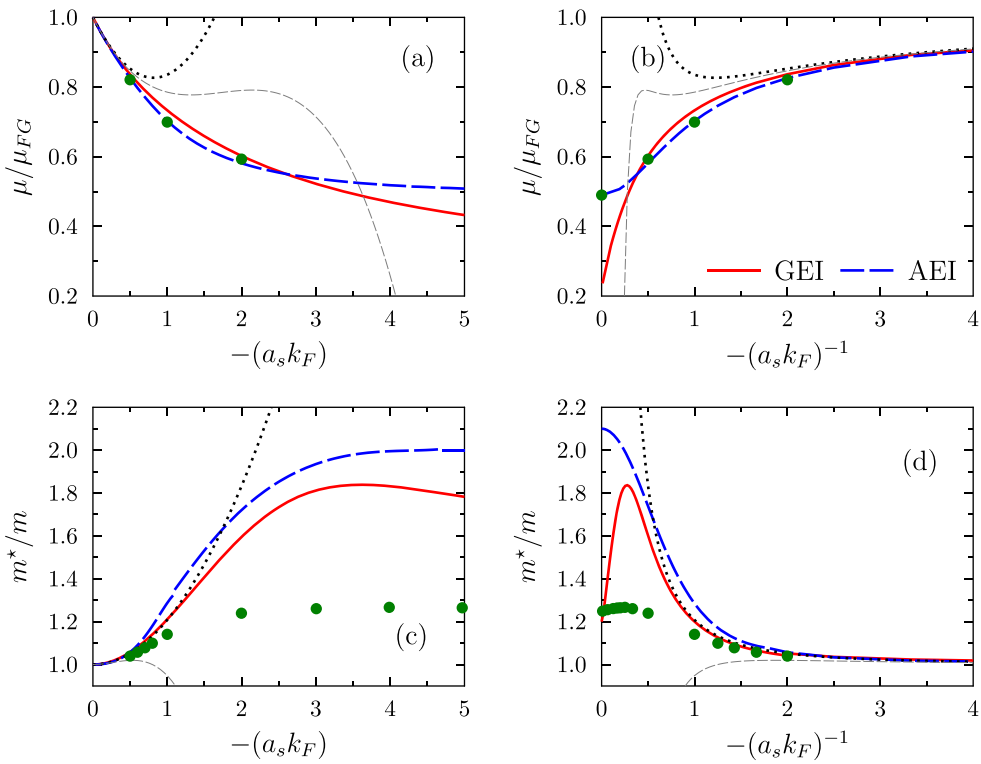

Figure 4. Chemical potential and effective mass as a function of $(a_s k_F)$ (panels (a) and (c)) or $-(a_s k_F)^{-1}$ (panels (b) and (d)) obtained with the GEI (red solid line) and AEI (blue dashed line) approximations. Result of the second order (Galitskii formula) and third order expansion [71] in $(a_s k_F)$ are shown with black dotted and thin gray dashed lines, respectively. The green circles correspond to the result of the BHF calculations of [18].

second or third order perturbation theory. We also observe that the effective mass, as well as the chemical potential, obtained with each other strongly depend on the selected diagrams.

A last important remark for the discussion below is that the expression of the resummed self-energies obtained either from pp ladders or combined pp and hh ladders resummations are *consistent* with the GEI and AEI approximations given by equations (5) and (6), respectively. Consistent means here that they respect the Hugenholtz-van-Hove (HvH) theorem [98]. This theorem (at zero temperature) states that the single-particle energy, given by equation (20), evaluated at the Fermi surface ($k = k_F$) is equal to the chemical potential of the systems. Using the thermodynamical relation between the chemical potential and the ground state energy, $\mu = \partial E/\partial N|_V$, where V is the unit volume, the HvH theorem leads to:

$$\frac{\mu}{\mu_{FG}} = \frac{E}{E_{FG}} + \frac{k_F}{5}\frac{\partial E/E_{FG}}{\partial k_F} = 1 + \frac{\mathrm{Re}\,\{\Sigma(k_F)\}}{\mu_{FG}}. \tag{21}$$

This equation gives a strong constraint between the energy and single-particle potential at $k = k_F$.

We have seen here that the resummation of diagrams is only a semi-success to predict quasi-particle properties. More specifically, the effective mass deviates rather rapidly from the

expected result as $|a_s k_F|$ increases. Although their predictive power is limited, the AEI and GEI approximation can serve as a guidance to provide simplified expressions of the self-energy that will be useful latter on the DFT context. We discuss below two approaches to obtain compact expression of the single-particle potential.

4.1. Partial phase-space (PPS) approximation for the self-energy

As we have seen in section 3.1, the phase-space approximation, by avoiding the estimates of rather complex integrals, automatically led to simplified expressions for the resummed energy that turned out to be rather useful in practice [8, 24, 46]. The goal here is to develop an equivalent method directly at the self-energy level.

The first difference compared to the energy is that the phase-space approximation should not be made on all variables because the self-energy depends on k (or p). In the following, starting from expression (14), for any function X that depends on the variable (s, t, p), we will introduce the two averages:

$$\langle X\rangle_p^< \equiv \int_0^1 s^2 \mathrm{d}s \int_0^{\sqrt{1-s^2}} t\mathrm{d}t\, X(s, t, p), \tag{22}$$

$$\langle X\rangle_p^> \equiv \int_0^{(1+p)/2} s^2 \mathrm{d}s \int_0^{(1+p)/2} t\mathrm{d}t X(s, t, p), \tag{23}$$

that denotes PPS approximation at fixed value of p, respectively, relevant for $p < 1$ and $p > 1$. With these notations, equation (14) writes:

$$\frac{\Sigma(k)}{\mu_{\mathrm{FG}}} = \Theta(k_F - k)\langle \mathcal{S}\rangle_p^< + \Theta(k - k_F)\langle \mathcal{S}'\rangle_p^>.$$

Expressions of the PPS for some functions are given in appendix B.2.

Starting from these expressions, our goal is to provide for the self-energy a phase-space approximation similar to the one for the energy given in section 3.1. Following the strategy we used previously, we will impose the approximate form to fulfill specific constraints:

(i) **Low density limit:** We will always impose that the self-energy matches the exact self-energy in the low density limit up to a certain order in $(a_s k_F)$.
(ii) **Large $(a_s k_F)$ limit:** We also seek for expressions that do not diverge in the limit $|a_s k_F| \to +\infty$.
(iii) **Consistency with the HvH theorem:** While it is not *a priori* absolutely necessary, in some cases, we will in addition impose that the self-energy we obtained should be consistent with either the GPS or the APS energy. Again, consistency means here that the considered self-energy and the energy obtained through phase-space approximation leads to the same chemical potential using equation (21). Note that the latter condition is more constraining than the condition (i) and (ii). In particular, since the energy already has the constraints (i) and (ii), they will be automatically fulfilled when (iii) is explicitly imposed.

In the following, we present two strategies to get approximate self-energies using PPS. In the first strategy called hereafter *simple* PPS approximation, we only impose conditions (i) and (ii). While in the second strategy, that would be called *consistent* PPS, the form of the energy deduced will also be constrained to one of the PS approximation discussed in section 3.1 by requiring the HvH theorem to hold.

4.2. Simple PPS approximation for the self-energy

We illustrate here a first simple strategy we can follow to impose (i) and (ii) avoiding complicated integrals. Our starting point is equation (14). As an illustration, we consider the specific case of the pp diagrams resummation and concentrate on the real part $U_{\rm pp}$ of the self-energy with $p < 1$. Starting from the expressions given in appendix B, a direct expansion of the denominator in $(a_s k_{\rm F})$ gives:

$$\frac{U_{\rm pp}(k)}{\mu_{\rm FG}} = \sum_{n=1}^{\infty} (a_s k_{\rm F})^n \Phi_n(p), \tag{24}$$

where the $\Phi_n(p)$ are given in terms of a PPS in the appendix by equation (B.10). For instance $\Phi_1(p) = 4/3\pi$ while the expression of $\Phi_2(p)$ is given by equation (B.1). In the following, we will often use the second order approximation:

$$U_{\rm pp}(k)/\mu_{\rm FG} = 4/3\pi(a_s k_{\rm F}) + \Phi_2(p)(a_s k_{\rm F})^2 + \mathcal{O}(a_s k_{\rm F})^3 \tag{25}$$

as a reference for the low density limit. Let us assume that we seek for an approximate form of the self-energy that matches the expansion (24) up to second order in $(a_s k_{\rm F})$ while being non-divergent at large value of a_s. Guided by the approximation made for the energy, one might simply use a Padé[1/1] approximate form:

$$\frac{U_{\rm pp}(k)}{\mu_{\rm FG}} \simeq \frac{4}{3\pi} \frac{(a_s k_{\rm F})}{1 - (a_s k_{\rm F})\frac{3\pi}{4}\Phi_2(p)}. \tag{26}$$

Note that, guided by the APS expression, a similar expression can be obtained that approximate the AEI. From these expressions and using the expansion of $\Phi_2(p)$ given by equation (18), we immediately see that the low density limit of the chemical potential and effective mass given by equation (19) are recovered. In addition starting from the expression of $\mu(k_{\rm F}) = \mu_{\rm FG} + U_{\rm pp}(k_{\rm F})$, the corresponding form of the energy in infinite systems can be obtained using the relationship:

$$\frac{E}{N} = \frac{1}{\rho}\frac{g}{2\pi^2}\int_0^{k_{\rm F}} k_{\rm F}'^2 \mu(k_{\rm F}') {\rm d}k_{\rm F}', \tag{27}$$

that can easily be obtained from the definition of μ as a partial derivative of the energy with respect to the particle number.

We compare in figure 5 the dependences of the chemical potential and effective mass obtained with the simple GPS approximation for the single-particle potential, respectively, as a function of $-(a_s k_{\rm F})$ or $-(a_s k_{\rm F})^{-1}$. By construction, contrary to an approximation where the self-energy is truncated at a given order in $(a_s k_{\rm F})$, simple GPS leads both to a smooth and converging behavior of these quantities up to infinite values of a_s. These approximated self-energies also reproduce correctly the low density limit. We see in particular that the chemical potential obtained with the simple PPS approximation follows closely the one of the original GEI result. We note also that the effective mass is more affected by the phase-space approximation. It turns out to be slightly lower compared to the GEI case and closer qualitatively to the BHF results up to $-(a_s k_{\rm F}) \simeq 3$. Not surprisingly, as in the original result obtained by direct integration, the large $|a_s k_{\rm F}|$ limit is not correctly accounted for. One difference we have observed however is that the dependence of $U_{\rm pp}(k)$ given by equation (26) close to unitarity remains very smooth and does not present the bumps seen in figure 3.

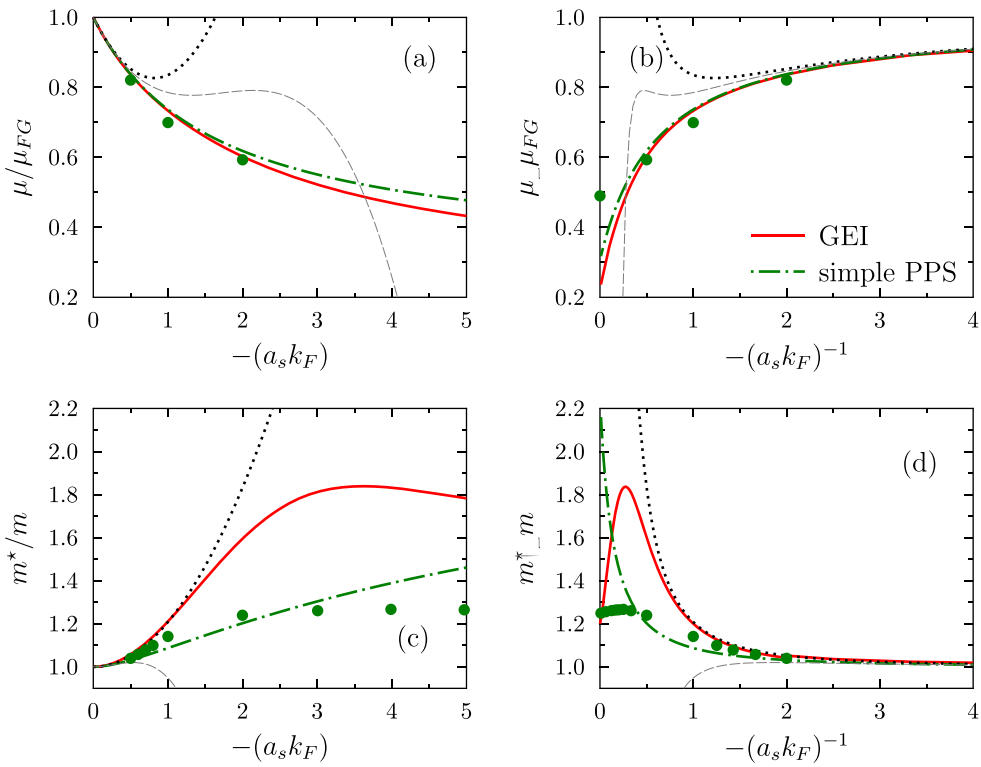

Figure 5. Comparison of the chemical potential (panels (a) and (c)) and effective mass (panels (b) and (d)) obtained with the simple PPS approximation given by equation (26) (green dot-long dashed line) and the original GEI result (red solid line). For comparison, the BHF results [18] are also shown (green circles).

4.3. PPS with the HvH theorem constraint: illustration with the GPS functional for $k < k_F$

The simple PPS approximation has some advantages. Among them, we note that the direct strategy used in previous sections automatically leads to the correct low density limit while the resulting single-particle potential $U_{\rm pp}$ has a rather compact expression. We also saw that it gives quite reasonable behavior much beyond the perturbative regime. One drawback is that the corresponding energy obtained by direct integration through equation (27) turns out to be more complex than typically the GPS and/or APS functionals given by equations (11) or (13). For this reason, we explored a different strategy that consists directly in imposing the constraint (iii), i.e. the energy obtained when applying equation (21) should match a pre-selected expression of the energy (the APS, GPS expressions for instance). In practice, this strategy is much less straightforward since the chemical potential is imposed whatever the value of $k_{\rm F}$ and a_s. It however has the direct advantage that all nice properties that were obtained at the energy level are automatically incorporated in the single-particle potential.

Our starting point is to pre-suppose that we already know the expression of the energy in terms of $(a_s k_{\rm F})$. As an illustration, we consider below that the energy should match the GPS energy given by equation (11) obtained by the pp ladder approximation. From the imposed energy, and using equation (21), we obtained that the potential at $k = k_{\rm F}$ should verify:

$$\frac{\mu}{\mu_{\rm FG}} = 1 + \frac{U_{\rm pp}(k_{\rm F})}{\mu_{\rm FG}} = 1 + \frac{\frac{4}{3\pi}(a_s k_{\rm F})}{1 - \frac{9\pi}{14}(a_s k_{\rm F})\Phi_2(1)} + \frac{\frac{1}{7}(a_s k_{\rm F})^2\Phi_2(1)}{\left[1 - \frac{9\pi}{14}(a_s k_{\rm F})\Phi_2(1)\right]^2},$$

where we have used the expression of $\Phi_2(1)$ given by equation (18) directly recognized in the chemical potential. From this, we see that imposing the HvH theorem at $k = k_{\rm F}$ (or $p = 1$) gives us a strong guidance on the single-particle potential for $k \neq k_{\rm F}$ (or $p \neq 1$). The simplest approximation that could be directly inferred from μ to obtain the potential consists in replacing $\Phi_2(1)$ by $\Phi_2(p)$, i.e.:

$$\frac{U_{\rm pp}(k)}{\mu_{\rm FG}} = \frac{\frac{4}{3\pi}(a_s k_{\rm F})}{1 - \frac{9\pi}{14}\Phi_2(p)(a_s k_{\rm F})} + \frac{\frac{1}{7}\Phi_2(p)(a_s k_{\rm F})^2}{\left[1 - \frac{9\pi}{14}\Phi_2(p)(a_s k_{\rm F})\right]^2}. \tag{28}$$

The present single-particle potential presents several specific properties:

- First, similarly to the simple PPS approach presented in previous section, its expansion to second order in $(a_S k_{\rm F})$ matches the exact result for low density Fermi gas.
- It also has automatically a non-divergent behavior in the limit $|a_s k_{\rm F}| \to +\infty$. Due to the HvH theorem constraint, the associated limit is compatible with the value of the associated Berstch parameter, $\xi_{\rm GPS}$ in the present illustration.
- The form of the single-particle potential turns out to be slightly more complicated than in the simple PPS approximation, equation (26). It is worth mentioning however that this form has strong similarities with the single-particle potential obtained by *pp* ladder approximation (see equation (B.7)), in particular with the presence of two terms with similar $(a_s k_{\rm F})$ dependence as in equation (28).
- Last, we note that the HvH constraint solely does not uniquely define the form of the potential $U_{\rm pp}$. Indeed, we can fulfill this constraint and keep all above mentioned properties using for instance the generalized formed:

$$\frac{U_{\rm pp}(k)}{\mu_{\rm FG}} = \frac{(4/3\pi)(a_s k_{\rm F})}{1 - (3\pi/4)\Phi_2(p)X(p)(a_s k_{\rm F})} + \frac{\Phi_2(p)[1 - X(p)](a_s k_{\rm F})^2}{[1 - (3\pi/4)\Phi_2(p)X(p)(a_s k_{\rm F})]^2}, \tag{29}$$

where the only constraint on $X(p)$ is that $X(1) = 6/7$. Again this flexibility should be seen as a positive point since it might be used to impose additional constraints latter on. In the following, we will generically denotes the potential given by equation (29) simply by $U_{{\rm GPS}_X}$ and refer to it as the ${\rm GPS}_X$ approximation, while the case $X(p) = 6/7$, leading to equation (28) is simply called GPS approximation for the single-particle potential and is noted as $U_{\rm GPS}$. Unless specified, results presented below will be obtained in the GPS approximation.

Equivalent strategy can be followed starting from the APS approximation. Imposing the HvH theorem consistent with the APS approximation for the energy, we end up with the following expression for the single-particle potential:

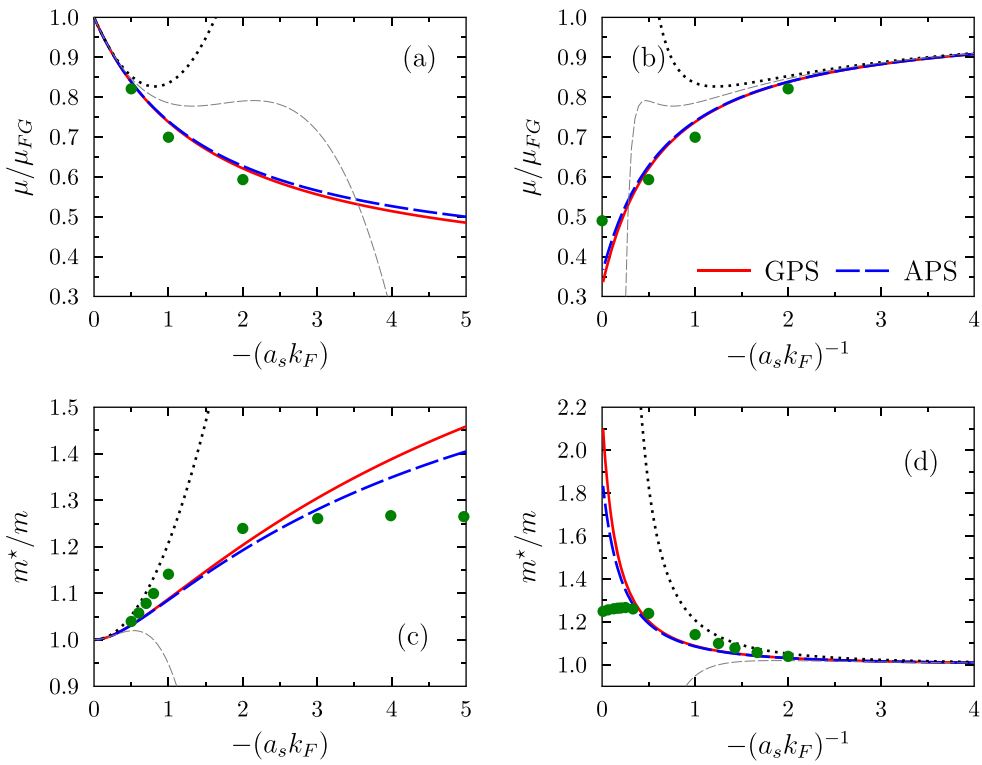

Figure 6. Chemical potential and effective mass as a function of $(a_s k_F)$ (panels (a) and (c)) or $-(a_s k_F)^{-1}$ (panels (b) and (d)) obtained with the GPS (red solid line) and APS (blue dashed line) approximations. In panels (a) and (c), result of the second order (Galitskii formula) and third order expansion [71] in $(a_s k_F)$ are shown with back dotted and thin gray dashed lines, respectively. The green circles correspond to the result of the BHF calculations of [18].

$$\frac{U_{\mathrm{APS}_X}(k)}{\mu_{\mathrm{FG}}} = \frac{(2/9\pi)a_s k_{\mathrm{F}}}{[1-(9\pi/4)\Phi_2(p)X(p)a_s k_{\mathrm{F}}]^2 + [(5/24)a_s k_{\mathrm{F}}]^2} + \frac{16}{3\pi}\arctan\left(\frac{(5/24)a_s k_{\mathrm{F}}}{1-(9\pi/10)\Phi_2(p)[1-X(p)]a_s k_{\mathrm{F}}}\right). \tag{30}$$

This approximation is called APS_X hereafter. The only constraint on the function $X(p)$ is now $X(p=1)=2/7$. If we assume that this function is constant for all p, approximation called simply APS hereafter, we end up with the single-particle potential:

$$\frac{U_{\mathrm{APS}}(k)}{\mu_{\mathrm{FG}}} = \frac{(2/9\pi)a_s k_{\mathrm{F}}}{[1-(9\pi/14)\Phi_2(p)a_s k_{\mathrm{F}}]^2 + [5a_s k_{\mathrm{F}}/24]^2} + \frac{16}{3\pi}\arctan\left(\frac{5a_s k_{\mathrm{F}}/24}{1-(9\pi/14)\Phi_2(p)a_s k_{\mathrm{F}}}\right). \tag{31}$$

Again, all constraints (i)–(iii) are respected and whatever the explicit form of $X(p)$, in the infinite scattering length limit, we obtain the APS value for the Bertsch parameter.

The chemical potential and effective mass dependence in $(a_s k_{\mathrm{F}})$ obtained with the consistent GPS and APS scheme are displayed in figure 6, respectively, as a function of $-(a_s k_{\mathrm{F}})$

or $-(a_s k_F)^{-1}$. The conclusions are similar as for the simple GPS case presented previously, i.e. the low density limit (respectively Lee-Yang and Galitskii formula) are properly reproduced by construction. The BHF results is reproduced qualitatively up to $-(a_s k_F) \simeq 3$ while the perturbative expansion breaks down around $-(a_s k_F) = 0.5$. We note however that the result of the consistent APS approximation is slightly worse compared to the original AEI as far as the chemical potential is concerned.

5. Quadratic and quartic approximation for the single-particle potential

Our targeted goal here is to provide DFT inspired by the many-body resummation technique presented above. The clear advantage to start from the self-energy level instead of the energy itself is that direct connections can be made between the self-energy and the Fermi Liquid theory. This was illustrated previously with the chemical potential and the effective mass. Such quantities are also standardly obtained with Energy Density Functionals for instance used in the nuclear physics context, like Skyrme or Gogny EDFs. Empirical functionals, especially the functionals derived using Skyrme like contact interactions lead to very simple single-particle potentials (see discussion below) with polynomial dependence in k. For instance, the original parameterization proposed in [2] leads simply to quadratic dependence of the single-particle potential in infinite matter. Novel generations of Skyrme EDF have been proposed leading to quartic or higher-order dependence in the momentum [99–101]. The justification that such simple approximation can contain important physical aspects can be found in [57]. The different single-particle potentials obtained in previous section presents rather complex density and momentum dependence. However, starting from the PPS approximation, one might obtain a systematic polynomial expansion to a given order in k. For this, we approximate the self-energy obtained by assuming a polynomial form. We introduce the following expansion:

$$U(k) \simeq U_0(k_F) + U_2(k_F)(k/k_F)^2 + U_4(k_F)(k/k_F)^4 + \cdots \tag{32}$$

This polynomial expansion, truncated at an appropriate order will not only be useful to make contact with empirical DFT but will also enable to obtain practical DFT for finite systems based on the present approach.

5.1. Quadratic approximation for the self-energy

The simplest approximation that is also certainly the most highlighting one for the present discussion is to consider quadratic single-particle potential, i.e. keeping only U_0 and U_2 in equation (32). Only two constraints are then needed to obtain U_0 and U_2. One possibility is to impose that some of the quasi-particle properties are exactly recovered. For instance, imposing the chemical potential and the effective mass to be the same as the original ones obtained with one of the PPS approximation leads to:

$$1 + \frac{U_0(k_F)}{\mu_{FG}} + \frac{U_2(k_F)}{\mu_{FG}} = \frac{\mu(k_F)}{\mu_{FG}}, \quad 1 + \frac{U_2(k_F)}{\mu_{FG}} = \frac{m}{m^*(k_F)},$$

giving finally:

$$\frac{U(k)}{\mu_{FG}} = \left[\frac{\mu(k_F)}{\mu_{FG}} - \frac{m}{m^*(k_F)}\right] + \left[\frac{m}{m^*(k_F)} - 1\right]\left(\frac{k}{k_F}\right)^2. \tag{33}$$

Since they are used as constraint, the present method automatically insures that the quasi-particle properties are preserved even if a simplified expansion is used for $U(k)$. Since the

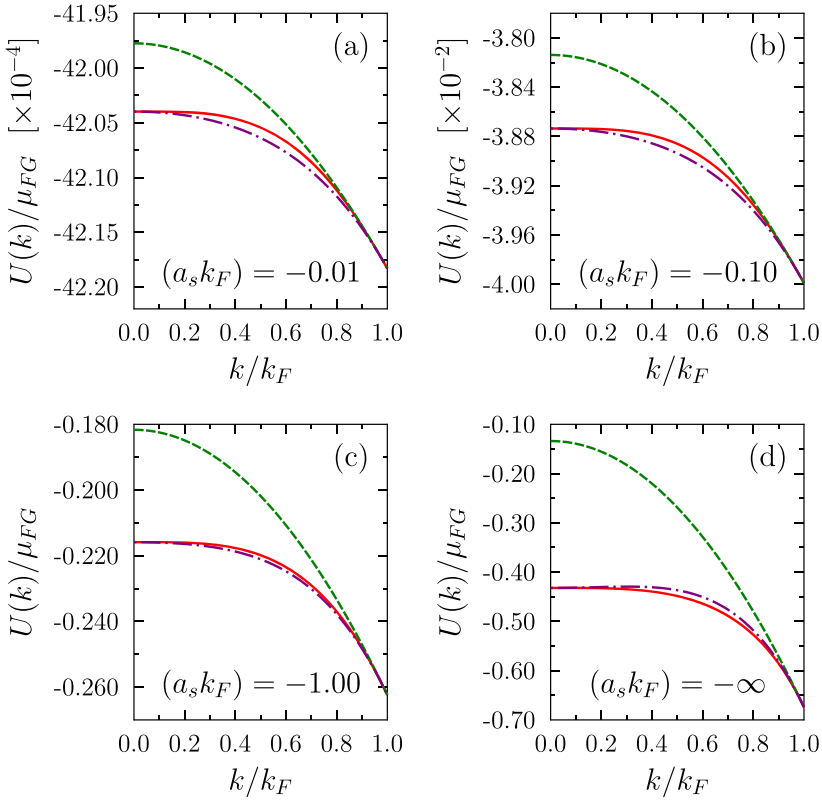

Figure 7. Momentum dependence of the approximated self-energy for $-(a_s k_F) = 0.01$ (a), 0.1 (b), 1 (c) and ∞ (d) obtained with the GPS approximation (red solid line). In each panel, the corresponding quadratic or quartic approximation are shown, respectively, by the green dashed line and purple long-short dashed line.

chemical potential is also constrained, due to the relationship (27), the energy of the system will also be preserved. Said differently, the GPS (resp. APS) approximation for the self-energy combined with the polynomial approximation of $U(k)$ will lead to the GPS (resp. APS) reference energy given by equation (11) (resp. (13)). This does not necessarily imply that the potentials are similar, however by construction, they should become identical as k becomes close to k_F. We compare in figures 7 and 8 for the GPS and APS cases, the original GPS and APS potentials given by equations (28) and (31) respectively, with their quadratic approximations for different values of $(a_s k_F)$. We clearly see in this figure that the value and the slope of $U(k)$ at $k = k_F$ that are, respectively, linked to the chemical potential and the effective mass are identical. However some differences are observed as k/k_F goes to zero. This also implies that some deviations occur with the second-order expansion of the self-energy given by equation (25) when the quadratic form of the potential is used in the low density limit. However, this approximation still leads to the proper behavior given by equation (19) in this limit.

The difference observed between the original GPS or APS approximations and the quadratic expansion given by equation (33) is further illustrated in figure 9 where we display the single-particle energy obtained in different cases at $k = 0$.

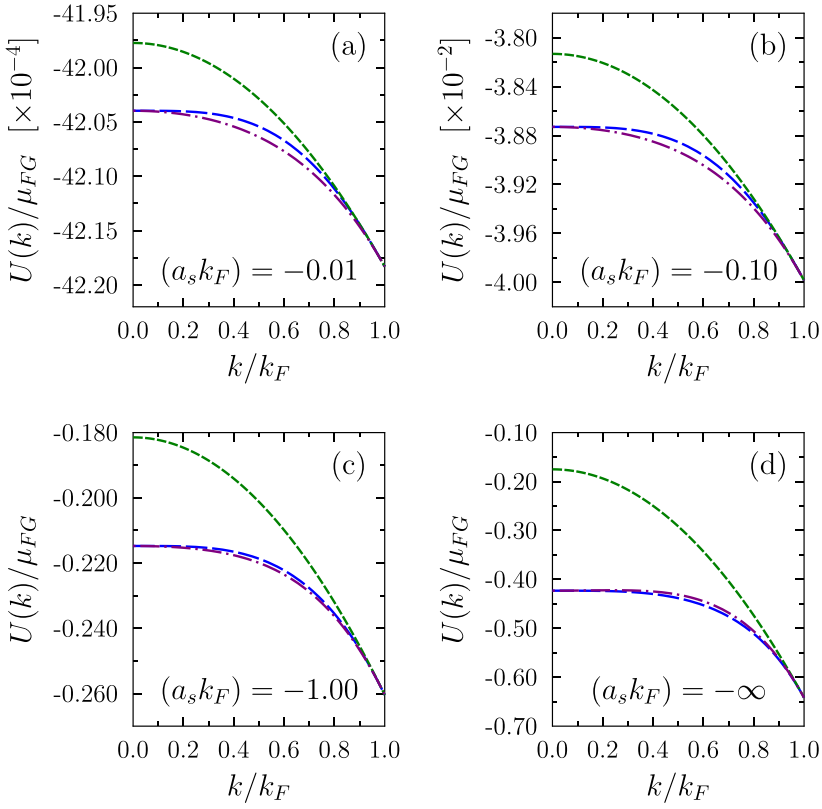

Figure 8. Same as figure 7 for the APS approximation. The reference APS curve is now shown with a blue long-dashed line.

5.2. Quartic approximation for the self-energy

The agreement between the original potential and the polynomial expansion can be significantly improved simply by going to a quartic form of the potential, i.e. by truncating the expansion (32) to the next order. Then, the three parameters can be adjusted by adding to the chemical potential and effective mass constraint, the additional constraint that the value of $U(k)$ at $k = 0$ is identical to the one of the original GPS and APS approximation. We see in figures 7 and 8, respectively, for the GPS and APS cases, that the quartic approximation significantly improves the global shape of the potential compared to the original PPS approximation.

6. Discussion on future developments towards non-empirical DFT for systems with anomalously large scattering length

In the present work, we focused our attention to infinite systems where the interaction is dominated by the s-wave channel and more specifically the s-wave scattering length. We decided a specific strategy, starting from a well-defined many-body technique to obtain energies written as a functional of $(a_s k_F)$. The energy can then be directly interpreted as a function of the one-body density ρ leading to a DFT for homogeneous system. These DFTs

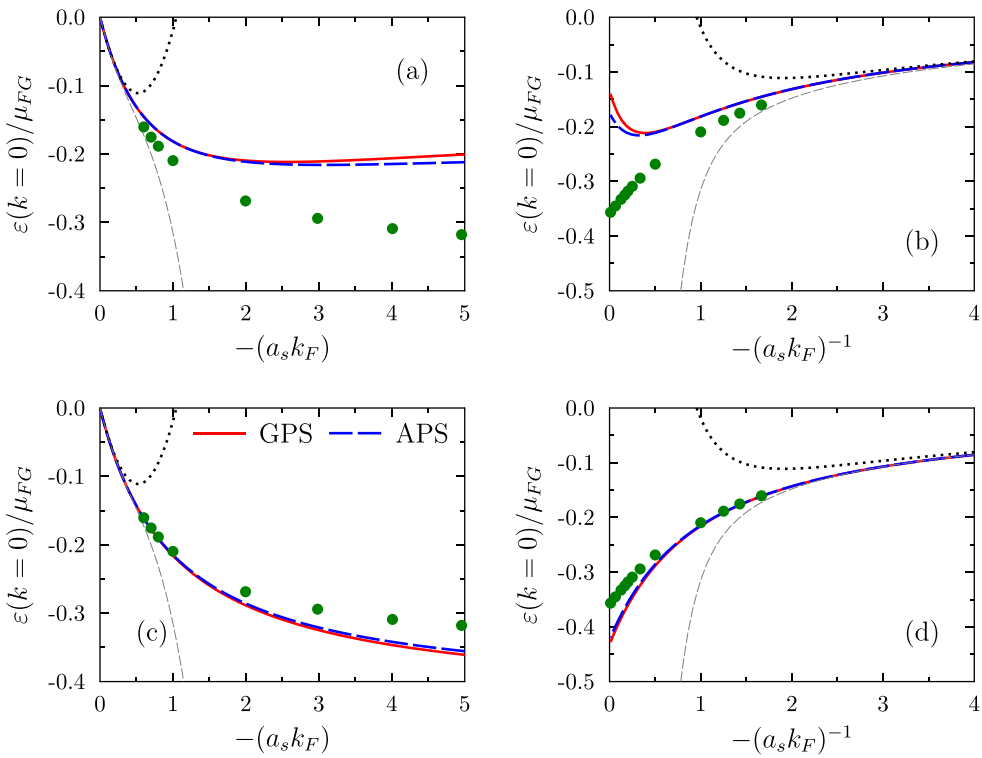

Figure 9. The single-particle energy $\varepsilon(k=0)$ at zero-momentum obtained from the GPS (red solid line) and APS (blue dashed line) single-particle potentials as a function of $-(a_s k_F)$ (panels (a) and (c)) or $-(a_s k_F)^{-1}$ (panels (b) and (d)). In panels (a) and (b) (resp. (c) and (d)) the results obtained using a quadratic (resp. quartic) approximation are shown in all panels by red solid line (GPS case) and blue dashed line (APS case). Note that in the quartic approximation, by construction (see text) the value of $\varepsilon(k=0)$ is equal to the original APS or GPS value. The black dotted line and gray dashed line correspond, respectively, to the value obtained from a quartic or quadratic approximation starting from the second order (equation (25)) or third order [71] expansion of the self-energy in $(a_s k_F)$, respectively. In all panels, the green circles correspond to the BHF results of [18].

automatically describe low density system and have *a priori* no free adjustable parameters. For this reason, we call them non-empirical. It is interesting to mention that the functionals obtained here can be interpreted as Padé approximation. Such Padé approximation was already used by Fayans [102] in the nuclear many-body problem with some success. There are however significant difference between the functional designed here and the one proposed in [102]. Besides the fact that the Fayans functional present a ratio of density dependent terms, one major difference is that it has been adjusted to reproduce the equation of state of neutron and symmetric matter. For instance, it does not reproduce the low density limit of interacting Fermi liquid. Obviously, the goal of empirical nuclear DFT [3] is more ambitious in the sense that it aims at reproducing globally nuclear system properties that results from a much more complicated interaction, including all channels, than the one we study here. Nevertheless, the possibility to get fully non-empirical DFT beyond the perturbative regime, even for a simple interaction, is an important step toward less empirical nuclear DFT.

We observe that the DFT we have obtained here still lacks from predictive power for instance for cold atoms close to unitary regime. Following [8, 46], one might eventually slightly relax the low density constraint and add specifically the unitary gas limit as a specific constraint. Unitary gas are indeed a well defined limit. This has been shown to provide very good reproduction of cold atoms from low to unitary limit or neutron matter up to $\rho \simeq 0.001\ \mathrm{fm}^{-3}$ is the effective range effects is included. We did not add this constraint in the present work due to the fact that our main priority was to obtain compact form of the self-energy with no *a posteriori* parameter adjusted and that there is a lack of clear guidance for normal unitary gas both for the single-particle potential and effective mass.

An important development that we are now pursuing is the possibility to apply the functional to finite Fermi systems. Let us assume that we start from one of the energy density functional given by equation (11) or equation (13), i.e. after PS approximation. Once the energy is written in terms of powers of k_{F}, this energy can directly be interpreted as a function of the local density ρ. For infinite systems, the local density is just a constant. A standard technique to export a DFT in infinite system to finite systems is to use a Local Density Approximation (LDA) where the equation (3) is first transformed into an integral over space of the energy density functional $E = \int \mathrm{d}^3 r\ \mathcal{E}(\boldsymbol{r})$. Here, $\mathcal{E}(\boldsymbol{r})$ contains the kinetic and the potential energy contributions that are both written in terms of the local density $\rho(\boldsymbol{r})$. This approach, that has some connections with the Thomas–Fermi approximation [103, 104], leads to functionals of the local density consistently with the Hohenberg–Kohn theorem [88]. Such direct mapping has initiated several novel ways to obtain DFT in the nuclear physics context [24, 43, 45] (for a review see [44]). Similar strategy is now currently used in a different context in order to incorporate quantum corrections that might stabilize quantum droplets [105, 106]. It is however well known that the simple LDA approach should be generalized by including properly the kinetic term as well as eventual gradient corrections. This is standardly done for instance in empirical nuclear DFT [3] and this was also one of the main motivations to extend our previous work from the energy to the self-energy.

To illustrate how a DFT beyond the LDA can be obtained from the present work, we assume that our starting points are the expression of $\mu(k_{\mathrm{F}})$ and $m^*(k_{\mathrm{F}})$ provided by one of the PPS approximation. We then introduce the quantity:

$$W(\rho) \equiv \frac{E}{N} - \frac{3}{5}\frac{\hbar^2 k_{\mathrm{F}}^2}{2m^*(\rho)}. \tag{34}$$

Note that the knowledge of $\mu(k_{\mathrm{F}})$ is sufficient to obtained the energy through the relation (27), thanks to the consistency requirement with the HvH theorem.

Following [104], we can show that this energy can be obtained from density functionals valid in both finite and infinite systems of the form:

$$E(\rho, \tau) = \int \left\{ \frac{\tau(\mathbf{r})}{2m^*(\rho)} + \rho(\mathbf{r}) W[\rho(\mathbf{r})] \right\} \mathrm{d}\mathbf{r}, \tag{35}$$

where the local density ρ and kinetic density τ entering in this equation are given by:

$$\rho(\mathbf{r}) = \sum_{i=1}^{N} |\varphi_i(\mathbf{r})|^2, \qquad \tau(\mathbf{r}) = \sum_{i=1}^{N} |\nabla\varphi_i(\mathbf{r})|^2. \tag{36}$$

The states $\{\varphi\}$ play the role of the Kohn–Sham state. The Schrödinger equation they fulfilled are obtained by minimizing the action $\mathcal{S} = E(\rho, \tau) - \sum_i \varepsilon_i |\nabla\varphi_i(\mathbf{r})|^2$ where ε_i are Lagrange multipliers that insures that single-particle are properly normalized to 1. Performing the variation of the action with respect to $\varphi_i^*(\mathbf{r})$ gives the set of self-consistent Kohn–Sham

equations:

$$\left\{-\vec{\nabla}\frac{1}{2m^*(\rho)}.\vec{\nabla} + U(\rho, \tau)\right\}\varphi_i(\mathbf{r}) = \varepsilon_i\varphi_i(\mathbf{r}), \tag{37}$$

where

$$U(\rho, \tau) = \frac{\hbar^2}{2}\tau\frac{\partial}{\partial\rho}\frac{1}{m^*(\rho)} + \frac{\partial}{\partial\rho}(\rho W(\rho)). \tag{38}$$

This approach gives a definite strategy to go beyond the LDA using the functionals proposed in the present work. Another interesting development for the future, especially to be able to use current nuclear DFT solvers, would be also to interpret the different terms as density dependent (t_0, x_0, t_1, x_1) Skyrme type parameters as it was done in [43, 45].

7. Summary

In the present work, we explore the possibility to start from a well-defined many-body approach based on the diagrammatic resummation technique and obtain approximate expressions both for the energy and/or the self-energy. While the present work is mainly focused on this topic, the ultimate goal is to use these approximate expressions as a guidance for proposing new DFT for Fermi systems beyond the perturbative regime. At the self-energy level, two simplifications are considered that might help in the DFT context. We first propose to use a PPS approximation leading to simpler density dependence of the self-energy and ultimately of the associated energy. We show that the PPS approximation can be made either by imposing the form of the energy simultaneously or not. In the former case, the constraint on the energy is made using the HvH theorem consistency. If the energy is not used as a constrained, the associated self-energy expression turns out to be simpler. In all cases, the self-energy of low density Fermi gas is properly recovered while a non-diverging limit is reached when $|a_s k_F| \to +\infty$ contrary to truncated perturbative many-body framework. It is found in general that the combination of a resummation technique with phase-space approximation can be used in a wider range of densities compared to many-body perturbation theory. We note however that without any adjustment, the functionals are not predictive in the unitary regime.

Besides the simplification introduced by the phase-space approximations, we note in general that the resulting energy and/or self-energy present both smoother behaviors that turn out to be qualitatively closer to the behavior calculated through BHF approach for non superfluid systems compared to a direct use of the resummation approach without PS approximation.

Guided by some phenomenological arguments commonly used for nuclei and also by the success of simple empirical functionals like the Skyrme DFT in nuclear systems, the single-particle potential is further simplified by assuming that the single-particle potential can be approximated by a quadratic or quartic polynomial in k. This second approximation is made in such a way that quasi-particle properties are preserved for all ($a_s k_F$). Again, this has the advantage that the low density limit of the chemical potential or the effective mass identifies automatically, respectively, with the Lee-Yang and Galitskii expression. We finally briefly discuss how the possibility to have analytical density dependent expressions of these quasi-particle properties can serve to design new DFTs. More generally, in view of the recent scientific emulation that followed the use of resummed formula for the energy [8, 24, 43, 44], the approximate expressions obtained in the present work can also be a strong guidance to

obtain semi-empirical or non-empirical functionals constrained at low density or at unitary or both.

The use of diagrammatic resummation leads to rather complex expressions in general. For this reason, we focused here the discussion on a rather simple case of a non-superfluid system with only one low energy constant, the s-wave scattering length focusing on the on-shell self-energy. In addition, an extension to include off-shell effects would be *a priori* desirable especially to describe the E-mass [107, 108]. Another natural extension of the present work is to include also the s-wave effective range r_e and/or p-wave scattering volume. The functional proposed in [8] and further discussed in [41, 46] already incorporate the effect of the effective range on the energy density functional. At leading order, one could simply add the present functional, however a proper treatment of the possible interference effects as well as effects beyond the leading order is needed if $(r_e k_{\mathrm{F}})$ becomes large for instance. This case happens for instance in nuclear system at saturation density. We did not consider here the treatment of the effective range together with large scattering length, however we mention that the work of [109, 110] can be use as a starting point.

Another important extension would be to include the effect of pairing correlations. As we mentioned in the introduction, a prerequisite for the present study is the possibility to obtain a compact expression of the energy after summing up selected diagrams to all orders in perturbations. By itself developing a perturbative approach on top of a quasi-particle vacua is possible (see for instance [111, 112]). However, even at second order, by replacing the 2p-2h energy by the 4 quasi-particle, the complexity of the integrals to be made increases significantly. As far as we know, such problem has not be solved analytically. An alternative to the analytical approach using a DFT guided by the present work would be simply to add *a posteriori* a pairing energy to the DFT. This procedure is standardly used for nuclei and would at least allow to extend to the so-called Superfluid LDA (SLDA) approach of [7] away from unitarity.

Acknowledgments

We thank H F Arellano, J Bonnard, M Grasso, A Gezerlis, C-J Yang for useful discussions at different stages of this work. This project has received funding from the European Union's Horizon 2020 research and innovation programme under Grant Agreement No. 654002.

Appendix A. Useful definitions and integrals

In the main text, several quantities are written as an integrals over the phase-space. For the sake of completeness, the different functions defined in the text as well as the different variable are summarized in this appendix. Note that a complete derivation of all equations can be found in [65].

Our starting point is the interaction matrix elements (1) written in momentum space as $\langle \boldsymbol{k_1}\boldsymbol{k_2}|V_{\mathrm{EFT}}|\boldsymbol{k_3}\boldsymbol{k_4}\rangle$ (note that, the spin is implicit and will lead to factors in the energy). Different functions appearing in the integrals for the energy and/or self-energy are written as a function of $s = |\boldsymbol{s}|$ and $t = |\boldsymbol{t}|$ where $\boldsymbol{s}$ and $\boldsymbol{t}$ are vectors defined through:

$$\boldsymbol{s} = \frac{\boldsymbol{k_1} + \boldsymbol{k_2}}{2k_{\mathrm{F}}}, \quad \boldsymbol{t} = \frac{\boldsymbol{k_1} - \boldsymbol{k_2}}{2k_{\mathrm{F}}}. \tag{A.1}$$

After proper treatment of the UV divergence and after averaging over vectors relative angles, it could be shown that the energy take the form (5) and (6), where I, F and R are given, respectively, by [40, 82]:

$$
\begin{aligned}
I(s,t) &= t\min\left[1;\left|\frac{1-s^2-t^2}{2st}\right|\right]\\
Y(s,t) &= 1+s+t\ln\left|\frac{1+s-t}{1+s+t}\right|+\frac{1-s^2-t^2}{2s}\ln\left|\frac{(1+s)^2-t^2}{1-s^2-t^2}\right|\\
F(s,t) &= Y(s,t)+\Theta(s-1)Y(-s,t)\\
R(s,t) &= Y(s,t)+Y(-s,t).
\end{aligned}
$$

A.1. Integrals used for phase-space average of the energy

The following integral are used to obtain the Phase-space averaged resummed expression for the energy:

$$
\begin{aligned}
\langle\langle 1\rangle\rangle &= \int_0^1 s^2\mathrm{d}s\int_0^{\sqrt{1-s^2}} t\mathrm{d}t = \frac{1}{15}\\
\langle\langle I\rangle\rangle &= \int_0^1 s^2\mathrm{d}s\int_0^{\sqrt{1-s^2}} t\mathrm{d}tI(s,t) = \frac{1}{72}\\
\langle\langle IR\rangle\rangle &= \int_0^1 s^2\mathrm{d}s\int_0^{\sqrt{1-s^2}} t\mathrm{d}tI(s,t)R(s,t) = \frac{1}{72}\times\frac{6}{35}(11-2\ln 2)\\
\langle\langle IF\rangle\rangle &= \int_0^1 s^2\mathrm{d}s\int_0^{\sqrt{1-s^2}} t\mathrm{d}tI(s,t)F(s,t) = \frac{1}{72}\times\frac{6}{35}(11-2\ln 2).
\end{aligned}
$$

Appendix B. Functions used in the self-energy

The two functions entering in the second-order self-energy, equation (16) are given by [90]:

$$
\begin{aligned}
\Phi_2(p) = {}& \frac{4}{15\pi^2}\frac{1}{p}\left\{11p+2p^5\ln\left|\frac{p^2}{p^2-1}\right|-10(p^2-1)\ln\left|\frac{p+1}{p-1}\right|\right\}\\
& -\frac{8}{15\pi^2}\frac{|2-p^2|^{5/2}}{p}\left\{\Theta(2-p^2)\ln\left|\frac{1+p\sqrt{2-p^2}}{1-p\sqrt{2-p^2}}\right|\right.\\
& \left.+\Theta(p^2-2)\cot^{-1}\sqrt{p^2-2}\right\},
\end{aligned}
\tag{B.1}
$$

$$
\begin{aligned}
\Omega_2(p) = {}& \Theta(1-p)\frac{(1-p^2)^2}{2\pi}\\
& -\Theta(p-1)\frac{2}{15\pi^2}\frac{1}{p}\{5p^2-7+2(2-p^2)^{5/2}\Theta(\sqrt{2}-p)\}.
\end{aligned}
\tag{B.2}
$$

Here, we use the Heaviside step function $\Theta(x)$ to shorten the notations.

B.1. Functions entering in the expression of the resummed self-energies

Particle–particle and hole–hole ladder diagrams resummation: In this case, we write the self-energy $\Sigma(k) = U(k) + \mathrm{i}W(k)$ as:

$$\frac{\Sigma(k)}{\mu_{\mathrm{FG}}} = \Theta(k_{\mathrm{F}} - k)\int_0^1 s^2\mathrm{d}s\int_0^{\sqrt{1-s^2}} t\mathrm{d}t\ [\mathcal{U}(s,t,p) + \mathrm{i}\mathcal{W}(s,t,p)] + \Theta(k - k_{\mathrm{F}})\int_0^{(1+p)/2} s^2\mathrm{d}s\int_0^{(1+p)/2} t\mathrm{d}t\ [\mathcal{U}'(s,t,p) + \mathrm{i}\mathcal{W}'(s,t,p)]$$

The different functions are given by ($k < k_{\mathrm{F}}$):

$$\frac{\mathcal{U}(s,t,p)}{\mu_{\mathrm{FG}}} = \frac{16(a_sk_{\mathrm{F}})^2 I_*(s,t)\widehat{R}(s,t,p) + (a_sk_{\mathrm{F}})\widehat{I_*}(s,t,p)[\pi - (a_sk_{\mathrm{F}})R(s,t)]}{[\pi - (a_sk_{\mathrm{F}})R(s,t)]^2 + [(a_sk_{\mathrm{F}})\pi I(s,t)]^2} - 16\widehat{R}(s,t,p)\delta(\pi/(a_sk_{\mathrm{F}}) - R(s,t))\Theta(1 - s^2 - t^2), \tag{B.3}$$

$$\frac{\mathcal{W}(s,t,p)}{\mu_{\mathrm{FG}}} = \frac{16\pi(a_sk_{\mathrm{F}})^2[\widehat{I_*}(s,t,p) - \widehat{I}(s,t,p)]I_*(s,t)}{[\pi - (a_sk_{\mathrm{F}})R(s,t)]^2 + [(a_sk_{\mathrm{F}})\pi I(s,t)]^2}. \tag{B.4}$$

and ($k > k_{\mathrm{F}}$):

$$\frac{\mathcal{U}'(s,t,p)}{\mu_{\mathrm{FG}}} = \frac{16(a_sk_{\mathrm{F}})^2 I_*(s,t)\widehat{R}(s,t,p) + (a_sk_{\mathrm{F}})\widehat{I_*}(s,t,p)[\pi - (a_sk_{\mathrm{F}})R(s,t)]}{[\pi - (a_sk_{\mathrm{F}})R(s,t)]^2 + [(a_sk_{\mathrm{F}})\pi I(s,t)]^2} - 16\widehat{R}(s,t,p)\delta(\pi/(a_sk_{\mathrm{F}}) - R(s,t))\Theta(1 - s^2 - t^2), \tag{B.5}$$

$$\frac{\mathcal{W}'(s,t,p)}{\mu_{\mathrm{FG}}} = -\frac{16\pi(a_sk_{\mathrm{F}})^2\widehat{I_*}(s,t,p)I(s,t)\Theta(s^2 + t^2 - 1)}{[\pi - (a_sk_{\mathrm{F}})R(s,t)]^2 + [(a_sk_{\mathrm{F}})\pi I(s,t)]^2}. \tag{B.6}$$

Note that, these results are equivalent those given by equations (18)–(21) of [82] except that the sign convention for the scattering length is different (i.e. $a_s \leftrightarrows -a_s$).

Particle–particle ladder diagrams only resummation: The resummed self-energy $\Sigma_{\mathrm{pp}}(k) = U_{\mathrm{pp}}(k) + \mathrm{i}W_{\mathrm{pp}}(k)$ is now given by:

$$\frac{\Sigma_{\mathrm{pp}}(k)}{\mu_{\mathrm{FG}}} = \Theta(k_{\mathrm{F}} - k)\int_0^1 s^2\mathrm{d}s\int_0^{\sqrt{1-s^2}} t\mathrm{d}t\ [\mathcal{U}_{\mathrm{pp}}(s,t,p) + \mathrm{i}\mathcal{W}_{\mathrm{pp}}(s,t,p)] + \Theta(k - k_{\mathrm{F}})\int_0^{(1+p)/2} s^2\mathrm{d}s\int_0^{(1+p)/2} t\mathrm{d}t\ [\mathcal{U}'_{\mathrm{pp}}(s,t,p) + \mathrm{i}\mathcal{W}'_{\mathrm{pp}}(s,t,p)].$$

The different functions are given by ($k < k_{\mathrm{F}}$):

$$\frac{\mathcal{U}_{\mathrm{pp}}(s,t,p)}{\mu_{\mathrm{FG}}} = \frac{16(a_sk_{\mathrm{F}})^2\widehat{F}(s,t,p)I_*(s,t)}{[\pi - (a_sk_{\mathrm{F}})F(s,t)]^2} + \frac{16(a_sk_{\mathrm{F}})\widehat{I_*}(s,t,p)}{\pi - (a_sk_{\mathrm{F}})F(s,t)} \tag{B.7}$$

$$\frac{\mathcal{W}_{\mathrm{pp}}(s,t,p)}{\mu_{\mathrm{FG}}} = \frac{16\pi(a_sk_{\mathrm{F}})^2[\widehat{I_*}(s,t,p) - \widehat{I}(s,t,p)]I_*(s,t)}{[\pi - (a_sk_{\mathrm{F}})F(s,t)]^2} \tag{B.8}$$

and ($k > k_F$):

$$\frac{\mathcal{U}'_{pp}(s,t,p)}{\mu_{FG}} = \frac{16(a_s k_F)^2 \widehat{F}(s,t,p) I_*(s,t)}{[\pi - (a_s k_F)F(s,t)]^2} + \frac{16(a_s k_F)\widehat{I}_*(s,t,p)\Theta(1-s^2-t^2)}{\pi - (a_s k_F)F(s,t)}$$
$$+ \frac{16(a_s k_F)[\pi - (a_s k_F)F(s,t)]\widehat{I}_*(s,t,p)\Theta(s^2+t^2-1)}{[\pi - (a_s k_F)F(s,t)]^2 + [(a_s k_F)\pi I(s,t)]^2}$$
$$\frac{\mathcal{W}'_{pp}(s,t,p)}{\mu_{FG}} = -\frac{16\pi(a_s k_F)^2 \widehat{I}_*(s,t,p) I(s,t)\Theta(s^2+t^2-1)}{[\pi - (a_s k_F)F(s,t)]^2 + [(a_s k_F)\pi I(s,t)]^2}. \tag{B.9}$$

The above quantities uses many more functions that are listed below:

$$I_*(s,t) = I(s,t)\Theta(1-s^2-t^2)$$
$$\widehat{I}(s,t,p) = \frac{1}{sp}\Theta(s+t-p)\Theta(p-|s-t|)\,\mathrm{sign}((1+p^2)/2 - s^2 - t^2)$$
$$\widehat{I}_*(s,t,p) = \frac{1}{sp}\Theta(s+t-p)\Theta(p-|s-t|)\Theta((1+p^2)/2 - s^2 - t^2)$$
$$\widehat{R}(s,t,p) = \frac{1}{sp}\ln\left|\frac{(s+p)^2-t^2}{(s-p)^2-t^2}\right|$$
$$\widehat{F}(s,t,p) = \frac{1}{sp}\left\{\Theta(2s-1)\Theta(2s-1-p)\ln\left|\frac{(s+p)^2-t^2}{(s-p)^2-t^2}\right|\right.$$
$$\left. + \Theta(p-|2s-1|)\ln\left|\frac{(s+p)^2-t^2}{(1+p^2)/2-s^2-t^2}\right|\right\}\Theta(1-p)$$
$$+ \frac{1}{sp}\left\{\Theta(p-2s-1)\ln\left|\frac{(s+p)^2-t^2}{(s-p)^2-t^2}\right|\right.$$
$$\left. + \Theta(2s+1-p)\ln\left|\frac{(s+p)^2-t^2}{(1+p^2)/2-s^2-t^2}\right|\right\}\Theta(p-1).$$

B.2. PPS average for different functions appearing in the self-energy

Starting from the expression (B.7), one can expand the potential as in equation (24) where the $\Phi_n(p)$ are given by:

$$\Phi_n(p) = \frac{16}{\pi^n}\langle \widehat{I}_* F^{n-1} + (n-1)F^{n-2}\widehat{F} I_*\rangle_p^<. \tag{B.10}$$

The PPS useful in the article are given by (note that some of them are independent on p):

$$\langle \widehat{I}_*\rangle_p^< = \frac{1}{12}, \quad \langle 1\rangle_p^< = \frac{1}{15}, \quad \langle I_*\rangle_p^< = \frac{1}{72}, \quad \langle \widehat{I}_* F + \widehat{F} I_*\rangle_p^< = \frac{\pi^2}{16}\Phi_2(p)$$

ORCID iDs

Antoine Boulet https://orcid.org/0000-0003-3839-6090
Denis Lacroix https://orcid.org/0000-0002-6296-2112

References

[1] Skyrme T H R 1959 *Nucl. Phys.* **9** 615
[2] Vautherin D and Brink D M 1972 *Phys. Rev.* C **5** 626
[3] Bender M, Heenen P-H and Reinhard P-G 2003 *Rev. Mod. Phys.* **75** 121
[4] Stone J and Reinhard P G 2007 *Prog. Part. Nucl. Phys.* **58** 587
[5] Schwenk A and Polonyi J 2012 *Renormalization Group and Effective Field Theory Approaches to Many-Body Systems* (Berlin: Springer)
Furnstahl R J EFT for DFT 133–91
Schäfer T Effective theories of dense and very dense matter 193–243
[6] Papenbrock T 2005 *Phys. Rev.* A **72** 041603(R)
[7] Bulgac A 2007 *Phys. Rev.* A **76** 040502
[8] Lacroix D 2016 *Phys. Rev.* A **94** 043614
[9] Chang S Y, Pandharipande V R, Carlson J and Schmidt K E 2004 *Phys. Rev.* A **70** 043602
[10] Bulgac A, Drut J and Magierski P 2008 *Phys. Rev.* A **78** 023625
[11] Forbes M M, Gandolfi S and Gezerlis A 2011 *Phis. Rev. Lett.* **106** 235303
[12] Gezerlis A and Carlson J 2008 *Phys. Rev.* C **77** 032801(R)
[13] Carlson J, Gandolfi S and Gezerlis A 2012 *Prog. Theor. Exp. Phys.* **2012** 01A209
[14] Forbes M M, Gandolfi S and Gezerlis A 2012 *Phys. Rev.* A **86** 053603
[15] Endres M G, Kaplan D B, Lee J-W and Nicholson A N 2013 *Phys. Rev.* A **87** 023615
[16] Haussmann R, Rantner W, Cerrito S and Zwerger W 2007 *Phys. Rev.* A **75** 023610
[17] Haussmann R, Punk M and Zwerger W 2009 *Phys. Rev.* A **80** 063612
[18] Doggen E V H and Kinnumen J J 2015 *Sci. Rep.* **5** 9539
[19] van Houcke K, Werner F, Kozik E, Prokof'ev N, Svistunov B, Ku M J H, Sommer A T, Cheuk L W, Schirotzek A and Zwierlein M W 2012 *Nat. Phys.* **8** 366
[20] Rossi R, Ohgoe T, Kozik E, Prokof'ev N, Svistunov B, Van Houcke K and Werner F 2018 *Phys. Rev. Lett.* **121** 130406
[21] Rossi R, Ohgoe T, Van Houcke K and Werner F 2018 *Phys. Rev. Lett.* **121** 130405
[22] Bender M, Bertsch G F and Heenen P-H 2005 *Phys. Rev. Lett.* **94** 102503
[23] Navarro Pérez R, Schunck N, Dyhdalo A, Furnstahl R J and Bogner S K 2018 *Phys. Rev.* C **97** 054304
[24] Yang C-J, Grasso M and Lacroix D 2016 *Phys. Rev.* C **94** 031301(R)
[25] Negele J W and Vautherin D 1972 *Phys. Rev.* C **5** 1472
[26] Negele J W and Vautherin D 1975 *Phys. Rev.* C **11** 1031
[27] Gebremariam B, Duguet T and Bogner S K 2010 *Phys. Rev.* C **82** 014305
[28] Stoitsov M, Kortelainen M, Bogner S K, Duguet T, Furnstahl R J, Gebremariam B and Schunck N 2010 *Phys. Rev.* C **82** 054307
[29] Carlsson B G and Dobaczewski J 2010 *Phys. Rev. Lett.* **105** 122501
[30] Gebremariam B, Bogner S K and Duguet T 2011 *Nucl. Phys.* A **851** 17
[31] Bogner S K, Furnstahl R J, Hergert H, Kortelainen M, Maris P, Stoitsov M and Vary J P 2011 *Phys. Rev.* C **84** 044306
[32] Dyhdalo A, Bogner S K and Furnstahl R J 2017 *Phys. Rev.* C **95** 054314
[33] Puglia S J, Bhattacharyya A and Furnstahl R J 2003 *Nucl. Phys.* A **723** 145
[34] Bhattacharyya A and Furnstahl R J 2005 *Nucl. Phys.* A **747** 268
[35] Yokota T, Yoshida K and Kunihiro T 2019 *Phys. Rev.* C **99** 024302
[36] Furnstahl R J, Steele J V and Tirfessa N 2000 *Nucl. Phys.* A **671** 396
[37] Furnstahl R J, Rupak G and Schäfer T 2008 *Ann. Rev. Nucl. Part. Sci.* **58** 1
[38] Hammer H-W and Furnstahl R J 2000 *Nucl. Phys.* A **678** 277
[39] Schäfer T, Kao C-W and Cotanch S R 2005 *Nucl. Phys.* A **762** 82
[40] Kaiser N 2011 *Nucl. Phys.* A **860** 41
[41] Lacroix D, Boulet A, Grasso M and Yang C-J 2017 *Phys. Rev.* C **95** 054306
[42] Zhang Y N, Bogner S K and Furnstahl R J 2018 *Phys. Rev.* C **98** 064306
[43] Grasso M, Lacroix D and Yang C-J 2017 *Phys. Rev.* C **95** 054327
[44] Grasso M 2018 *Prog. Part. Nucl. Phys.* **106** 256–311
[45] Bonnard J, Grasso M and Lacroix D 2018 *Phys. Rev.* C **98** 034319
[46] Boulet A and Lacroix D 2018 *Phys. Rev.* C **97** 014301
[47] Buraczynski M and Gezerlis A 2016 *Phys. Rev. Lett.* **116** 152501
[48] Buraczynski M and Gezerlis A 2017 *Phys. Rev.* C **95** 044309

[49] Ismail N, Buraczynski M and Gezerlis A 2019 *Phys. Rev. Lett.* **122** 152701
[50] Isaule F, Arellano H F and Rios A 2016 *Phys. Rev.* C **94** 034004
[51] Arellano H F, Isaule F and Rios A 2016 *Eur. Phys. J.* A **52** 299
[52] Huang K and Yang C N 1957 *Phys. Rev.* **105** 767
[53] Huang K, Yang C N and Luttinger J M 1957 *Phys. Rev.* **105** 776
[54] Lee T D and Yang C N 1957 *Phys. Rev.* **105** 1119
[55] Abrikosov A A and Khalatnikov I M 1958 *JETP* **6** 888
[56] Belyakov V A 1961 *JETP* **13** 850
[57] Fetter A L and Walecka J D 1971 *Quantum Theory of Many-Particle Systems* (New York: McGraw-Hill)
[58] Bollini C G and Giambiagi J J 1972 *Nuovo Cimento* B **12** 20
[59] Lepage G P 1997 arXiv:9706029 [nucl-th]
[60] Kaplan D B, Savage M J and Wise M B 1998 *Nucl. Phys.* B **534** 329
[61] Kaplan D B, Savage M J and Wise M B 1998 *Phys. Lett.* B **424** 390
[62] Phillips D R 1998 arXiv:9804040 [nucl-th]
[63] Birse M C 1998 arXiv:9804028 [nucl-th]
[64] Bedaque P F and van Kolck U 2002 *Annu. Rev. Nucl. Part. Sci.* **52** 339
[65] Boulet A 2019 *PhD Dissertation* Université Paris-Saclay in preparation
[66] Efimov V N and Amusya M Y 1965 *Sov. Phys. JETP* **20** 388
[67] Amusia M Y and Efimov V N 1968 *Ann. Phys. (NY)* **47** 377
[68] Baker G A 1971 *Rev. Mod. Phys.* **43** 479
[69] Bishop R F 1973 *Ann. Phys. (NY)* **77** 106
[70] Steele J V 2000 arXiv:0010066v2 [nucl-th]
[71] Platter L, Hammer H-W and Meissner U-G 2003 *Nucl. Phys.* A **714** 250
[72] Mecca A, Lovato A, Benhar O and Polls A 2015 *Phys. Rev.* C **91** 034325
[73] Mecca A, Lovato A, Benhar O and Polls A 2016 *Phys. Rev.* C **93** 035802
[74] Holt J W and Kaiser N 2017 *Phys. Rev.* C **95** 034326
[75] Kaiser N 2017 *Eur. Phys. J.* A **53** 104
[76] Wellenhofer C, Drischler C and Schwenk A 2018 arXiv:1812.08444 [nucl-th]
[77] Zwerger W (ed) 2012 *The BCS-BEC Crossover and the Unitary Fermi Gas* (*Lecture Notes Physics* vol 836) (Berlin: Springer)
[78] Chin C, Grimm R, Julienne P and Tiesinga E 2010 *Rev. Mod. Phys.* **82** 1225
[79] Day B D 1967 *Rev. Mod. Phys.* **39** 719
[80] Brandow B H 1967 *Rev. Mod. Phys.* **39** 771
[81] Bethe H A 1971 *Annu. Rev. Nucl. Sci.* **21** 93
[82] Kaiser N 2013 *Eur. Phys. J.* A **49** 140
[83] Navon N, Nascimbène S, Chevy F and Salomon C 2010 *Science* **328** 729
[84] Ku M J H, Sommer A T, Cheuk L W and Zwierlein M W 2012 *Science* **335** 563
[85] Baker G A Jr. 1999 *Phys. Rev.* C **60** 054311
[86] Heiselberg H 2001 *Phys. Rev.* A **63** 043606
[87] Adhikari S K 2008 *Phys. Rev.* A **77** 045602
[88] Hohenberg P and Kohn W 1964 *Phys. Rev.* **136** B864
[89] Kohn W and Sham L J 1965 *Phys. Rev.* **140** A1133
[90] Galitskii V M 1958 *JETP* **34** 104
[91] Galitskii V M and Migdal A B 1958 *JETP* **34** 96
[92] Rajaraman R and Bethe H A 1967 *Rev. Mod. Phys.* **39** 745
[93] Brown G E 1971 *Rev. Mod. Phys.* **43** 1
[94] Khodel V V and Saperstein E E 1982 *Phys. Rep.* **92** 183
[95] Landau L D 1957 *JETP* **3** 920
Landau L D 1957 *JETP* **3** 101
Landau L D 1959 *JETP* **3** 70
[96] Stewart J T, Gaebler J P and Jin D S 2008 *Nature* **454** 744
[97] Hahn T 2005 *Comput. Phys. Commun.* **168** 78
[98] Hugenholtz N M and van Hove L 1958 *Physica* **24** 363
[99] Raimondi F, Carlsson B G and Dobaczewski J 2011 *Phys. Rev.* C **83** 054311
[100] Davesne D, Pastore A and Navarro J 2014 *J. Phys. G: Nucl. Part. Phys.* **41** 065104
[101] Davesne D, Navarro J, Meyer J, Bennaceur K and Pastore A 2018 *Phys. Rev.* C **97** 044304
[102] Fayans S A 1998 *JETP Lett.* **68** 169

[103] Ring P and Schuck P 1980 *The Nuclear Many-Body Problem* (Berlin: Springer)
[104] Lipparini E 2008 *Modern Many-Particle Physics: Atomic Gases* (Singapore: World Scientific)
[105] Bulgac A 2002 *Phys. Rev. Lett.* **89** 050402
[106] Ferrier-Barbut I, Kadau H, Schmitt M, Wenzel M and Pfau T 2016 *Phys. Rev. Lett.* **116** 215301
[107] Jeukenne J P, Lejeune A and Mahaux C 1976 *Phys. Rep.* **25C** 83
[108] Mahaux C, Davis K T R and Satcher G R 1993 *Phys. Rep.* **224** 237
[109] Lacour A, Oller J A and Meissner U-G 2011 *Ann. Phys. (NY)* **326** 241
[110] Kaiser N 2012 *Eur. Phys. J.* A **48** 148
[111] Lacroix D and Gambacurta D 2012 *Phys. Rev.* C **86** 014306
[112] Ripoche J, Lacroix D, Gambacurta D, Ebran J-P and Duguet T 2017 *Phys. Rev.* C **95** 014326